

# Implicit Unitarity Bias in Tensor Factorization: A Theoretical Framework for Symmetry Group Discovery

**Dongsung Huh**

*Independent Researcher*

DONGSUNGHUH@GMAIL.COM

**Halyun Jeong**

*University at Albany, State University of New York*

HJEONG2@ALBANY.EDU

## Abstract

While modern neural architectures typically generalize via smooth interpolation, it lacks the inductive biases required to uncover algebraic structures essential for systematic generalization. We present the first theoretical analysis of HyperCube, a differentiable tensor factorization architecture designed to bridge this gap. This work establishes an intrinsic geometric property of the HyperCube formulation: we prove that the architecture mediates a fundamental equivalence between geometric alignment and algebraic structure. Independent of the global optimization landscape, we show that the condition of geometric alignment imposes rigid algebraic constraints, proving that the feasible collinear manifold is non-empty if and only if the target is isotopic to a group. Within this manifold, we characterize the objective as a rank-maximizing potential that unconditionally drives factors toward full-rank, unitary representations. Finally, we propose the Collinearity Dominance mechanism to link these structural results to the global landscape. Supported by empirical scaling laws, we establish that global minima are achieved exclusively by unitary regular representations of group isotopes. This formalizes the HyperCube objective as a differentiable proxy for associativity, demonstrating how rigid geometric constraints enable the discovery of latent algebraic symmetry.

**Keywords:** Symmetry Groups, Group Structure Discovery, Unitary Representations, Tensor Completion, Tensor Factorization, Implicit Inductive Bias

## 1. Introduction

Identifying latent algebraic structure—especially group structure—is a cornerstone of scientific discovery. Groups formalize the notion of symmetry, the fundamental principle that generalizes local observations into universal laws of nature (Noether, 1918). Indeed, the discovery of symmetry groups has been essential to the development of modern physics (Wigner, 1967; Gross, 1996).

In deep learning, this principle is operationalized through *Geometric Deep Learning* (Bronstein et al., 2021), which embeds *a priori* symmetries directly into the network architecture. While yielding superior generalization and sample efficiency (Cohen and Welling, 2016), this approach is brittle: it limits applicability when the underlying symmetry is unknown or mismatched with the data. In contrast, modern flexible architectures (e.g., Transformers) avoid these rigid constraints by imposing minimal symmetry assumptions (Vaswani et al., 2017). While capable of capturing complex patterns given vast amounts of data and compute, their lack of structural inductive bias exposes them to fundamental limitations, including low sample efficiency, susceptibility to *shortcut learning* (Geirhos et al., 2020), and a failure to generalize systematically (Lake and Baroni, 2018).

A central challenge is to reconcile these paradigms: to integrate flexible architectures with a high-level inductive bias that enables the *discovery of latent group structures* directly from data. However, automating this discovery is a significant technical hurdle. The discrete axioms of group

theory—particularly associativity—are inherently non-differentiable, making them incompatible with standard gradient-based optimization. Consequently, discovering these structures remains largely a manual endeavor, contingent upon prior domain knowledge.

The *HyperCube* model (Huh, 2025) proposes a differentiable relaxation of discrete group axioms by modeling algebraic operations via an *operator-valued tensor factorization*. The validity of this formulation is empirically substantiated by a strong inductive bias toward group structures, which manifests in two distinct phenomena:

1. *Bias toward Unitary Representations*: The learned factors exhibit a consistent preference for converging to full-rank, *unitary* representations.
2. *Bias toward Group Isotopes*: The model displays a structural bias toward recovering group isotopes from generic algebraic structures.

**Low-Rank vs. Unitarity Bias.** Our primary objective is to characterize the optimization landscape of HyperCube to elucidate the mechanism inducing these structural biases. Crucially, this inherent preference for **rank maximization** stands in sharp contrast to the **low-rank simplicity bias** prevalent in modern learning theory. In matrix completion, rank minimization is an *explicit* principle for generalization (Fazel et al., 2001; Candès and Recht, 2009; Candes and Tao, 2010). Similarly, matrix and tensor factorization (Gunasekar et al., 2017; Arora et al., 2019; Razin et al., 2021) and deep neural networks (Saxe et al., 2014; Jacot, 2022; Huh et al., 2023) exhibit an *implicit* bias toward minimum-rank solutions. While such biases enable generalization via **parsimonious interpolation**, HyperCube’s distinct preference for full-rank (unitary) structures marks a fundamental departure, suggesting a novel mechanism for **structural generalization**.

**Our Contributions.** The HyperCube model’s quartic objective  $\mathcal{H}$  subject to trilinear constraints induces a nonconvex landscape with non-compact gauge orbits, rendering direct global analysis intractable. To resolve this, we derive an *orthogonal decomposition*  $\mathcal{H} = \mathcal{B} + \mathcal{R}$ , isolating a tractable **collinear manifold** ( $\mathcal{R} = 0$ ) to establish the following:

- **Intrinsic Geometric-Algebraic Equivalence**: We prove that the HyperCube architecture mediates a fundamental correspondence between geometric factor alignment and associativity. We establish that the collinear manifold contains *feasible* factorizations **if and only if** the target is isotopic to a group (Section 4).
- **Unconditional Spectral Pressure**: Within this manifold, we characterize  $\mathcal{B}$  as a **rank-maximizing potential**. We prove it exerts a variational pressure that drives factors toward full-rank, unitary representations—identifying the regular representation as the unique structural optimum (Section 5).
- **Global Optimality via Collinearity Dominance**: To bridge these structural results to the global landscape, we propose the *Collinearity Dominance* mechanism. Supported by empirical observations, we prove that under this dominance, global minimizers are achieved exclusively by unitary representations of group isotopes (Section 6).
- **Differentiable Proxy for Associativity**: We provide empirical evidence that the HyperCube objective functions as a robust, differentiable proxy for algebraic associativity, enabling the discovery of latent symmetries where discrete axioms fail (Section 6.3).

## 2. Theoretical Framework

### 2.1. Algebraic Structures as Tensors

Let  $(Q, \circ)$  denote a finite set of  $n$  elements equipped with a binary operation  $\circ : Q \times Q \rightarrow Q$ . Its algebraic structure is represented as an order-3 structure tensor  $\delta \in \{0, 1\}^{n \times n \times n}$ :

$$\delta_{abc} := \mathbb{I}_{\{a \circ b = c\}}, \quad a, b, c \in Q, \quad (1)$$

which encodes the operation table (*i.e.*, *Cayley table*). We denote  $|\delta| := \sum_{a,b,c} \delta_{abc} = n^2$ . While [Huh \(2025\)](#) focused on recovering  $\delta$  from partial observations (*i.e.*, completion tasks ([Power et al., 2022](#))), we analyze the fully observed regime to rigorously characterize the optimization landscape.

**Groups and Quasigroups.** To simplify the algebraic analysis, we restrict our scope to *quasigroups*, a subset of binary operations where the equations  $a \circ x = b$  and  $y \circ a = b$  possess unique solutions. Equivalently, the structure tensor  $\delta$  encodes a Latin square (every slice is a permutation matrix). A *group* is then defined as a quasigroup that additionally satisfies the associativity property  $(a \circ b) \circ c = a \circ (b \circ c)$ .

**Supported Triples and Connectivity.** A triple  $(a, b, c)$  is called a supported triple if  $\delta_{abc} = 1$  (*i.e.*,  $a \circ b = c$ ). Unless otherwise noted, all indexed sums are restricted to these triples. Geometrically, these triples form the hyperedges of the support hypergraph (defined in [Appendix C](#)). For quasigroups, this structure is necessarily connected, which ensures that local algebraic constraints propagate globally.

### 2.2. HyperCube Model

**Notations.** For any  $X, Y \in \mathbb{C}^{n \times n}$ , define the normalized Frobenius inner product and norm

$$\langle X, Y \rangle := \frac{1}{n} \text{Tr}(X^\dagger Y), \quad \|X\|^2 := \langle X, X \rangle \quad (2)$$

so that  $\|U\|^2 = 1$  for any unitary  $U$ . Throughout,  $\dagger$  denotes the conjugate transpose.

**Operator-Valued Tensor Factorization.** HyperCube approximates the structure tensor  $\delta$  (1) via a trilinear product of parameter tensors  $A, B, C \in \mathbb{C}^{n \times n \times n}$ :

$$T_{abc}(\Theta) := \frac{1}{n} \text{Tr}(A_a B_b C_c), \quad \Theta := (A, B, C), \quad (3)$$

where  $A_a, B_b, C_c \in \mathbb{C}^{n \times n}$  denote the matrix slices indexed by  $a, b, c \in Q$ . Thus, the model captures the structural three-way interactions of the indices as the product of their matrix embeddings—*i.e.*, as a *composition of linear operators*.  $\Theta$  is said to **factorize**  $\delta$  if  $T(\Theta) = \delta$ .

**Optimization Objective.** HyperCube minimizes a *Jacobian-based regularization* objective

$$\mathcal{H}(\Theta) := \sum_{b,c \in Q} \|B_b C_c\|^2 + \sum_{c,a \in Q} \|C_c A_a\|^2 + \sum_{a,b \in Q} \|A_a B_b\|^2,$$

which penalizes the squared norm of the model’s Jacobian (3) with respect to the factors (*e.g.*,  $\partial T_{abc} / \partial A_a = (B_b C_c)^\dagger$ ). By exploiting the Latin-square property of  $\delta$ , the objective can be reformulated as a sum over supported triples, which facilitates our subsequent analysis:

$$\mathcal{H}(\Theta) = \sum_{a,b,c \in Q} \delta_{abc} (\|B_b C_c\|^2 + \|C_c A_a\|^2 + \|A_a B_b\|^2). \quad (4)$$

On the surface, such a Jacobian penalty simply promotes generic robustness by minimizing parameter sensitivity. In this work, we uncover the geometric mechanism by which this objective (4) induces a sharp bias toward rigid group structures through the factorization architecture (3).

### 3. Orthogonal Decomposition of $\mathcal{H}$

In this section, we derive the orthogonal decomposition  $\mathcal{H} = \mathcal{B} + \mathcal{R}$ , separating the objective into an **inverse-scale penalty**  $\mathcal{B}$  and a **directional misalignment penalty**  $\mathcal{R}$ . Throughout, we assume that every parameter slice has a positive norm ( $\|A_a\|^2, \|B_b\|^2, \|C_c\|^2 > 0$ ).

**Cauchy–Schwarz Bound.** The model (3) can be viewed as the inner product  $T_{abc} = \langle A_a^\dagger, B_b C_c \rangle$ . By Cauchy–Schwarz,  $|T_{abc}|^2 \leq \|A_a^\dagger\|^2 \|B_b C_c\|^2 = \|A_a\|^2 \|\partial T_{abc}/\partial A_a\|^2$ . Rearranging yields a local lower bound on the norm of the model Jacobian:

$$\left\| \frac{\partial T_{abc}}{\partial A_a} \right\|^2 \geq \frac{|T_{abc}|^2}{\|A_a\|^2},$$

with equality if and only if the factor  $A_a$  and the partial derivative  $\partial T_{abc}/\partial A_a$  are **collinear**. Aggregating these lower bounds across all Jacobian terms in (4) motivates the following definitions.

**Definition 1 (Inverse-Scale Penalty  $\mathcal{B}$ )** For any parameters  $\Theta$  and target  $\delta$ , define:

$$\mathcal{B}(\Theta; \delta) := \sum_{a,b,c} \delta_{abc} |T_{abc}|^2 \left( \frac{1}{\|A_a\|^2} + \frac{1}{\|B_b\|^2} + \frac{1}{\|C_c\|^2} \right). \quad (5)$$

**Definition 2 (Misalignment Penalty  $\mathcal{R}$ )** For any parameters  $\Theta$  and target  $\delta$ , define:

$$\mathcal{R}(\Theta; \delta) := \sum_{a,b,c} \delta_{abc} \left( \|\Delta_{abc}^{(A)}\|^2 + \|\Delta_{abc}^{(B)}\|^2 + \|\Delta_{abc}^{(C)}\|^2 \right) \geq 0. \quad (6)$$

where  $\Delta_{abc}^{(A)} := (B_b C_c)^\dagger - T_{abc}^* A_a / \|A_a\|^2$  with analogous definitions for  $\Delta_{abc}^{(B)}$  and  $\Delta_{abc}^{(C)}$ . These  $\Delta$  matrices represent the component of the Jacobian orthogonal to their respective factor slices; e.g.,  $\langle A_a, \Delta_{abc}^{(A)} \rangle = \langle A_a, (B_b C_c)^\dagger \rangle - T_{abc}^* \frac{\|A_a\|^2}{\|A_a\|^2} = T_{abc}^* - T_{abc}^* = 0$ .

**Lemma 3 (Decomposition of  $\mathcal{H}$ )** For any  $\Theta$  and target  $\delta$ , the objective (4) decomposes as

$$\mathcal{H}(\Theta) = \mathcal{B}(\Theta; \delta) + \mathcal{R}(\Theta; \delta). \quad (7)$$

Consequently,  $\mathcal{H}(\Theta) \geq \mathcal{B}(\Theta; \delta)$ , with equality if and only if  $\mathcal{R}(\Theta; \delta) = 0$ .

**Proof** Rearrange the definition of  $\Delta^{(A)}$  to express  $(B_b C_c)^\dagger = \frac{T_{abc}^*}{\|A_a\|^2} A_a + \Delta_{abc}^{(A)}$ . Squaring the norm and exploiting the orthogonality  $\langle A_a, \Delta_{abc}^{(A)} \rangle = 0$  yields:  $\|B_b C_c\|^2 = |T_{abc}|^2 / \|A_a\|^2 + \|\Delta_{abc}^{(A)}\|^2$ . Aggregating the Jacobian terms in (4) yields the decomposition  $\mathcal{H} = \mathcal{B} + \mathcal{R}$ .  $\blacksquare$

**Definition 4 (Collinear Manifold and Geometric Alignment)** The **collinear manifold** is the zero-set of the misalignment penalty:  $\mathcal{M}_\delta = \{\Theta \mid \mathcal{R}(\Theta; \delta) = 0\}$ . This condition is equivalent to **geometric alignment** (collinearity), satisfying the following identities for every supported triple  $(a, b, c)$ :

$$B_b C_c = T_{abc} \frac{A_a^\dagger}{\|A_a\|^2}, \quad C_c A_a = T_{abc} \frac{B_b^\dagger}{\|B_b\|^2}, \quad A_a B_b = T_{abc} \frac{C_c^\dagger}{\|C_c\|^2}. \quad (8)$$

## 4. Geometric Alignment Implies Algebraic Structure

This section establishes an **intrinsic geometric property** of the HyperCube formulation. Independent of the global landscape analysis (Section 6), we demonstrate that geometric alignment (8) imposes rigid algebraic constraints on the target  $\delta$ . Specifically, we establish a **fundamental equivalence**: the *feasible* collinear set is non-empty *if and only if* the target  $\delta$  is isotopic to a group. We prove this first for **unitary** factorizations, extending the result to the general case in Section 5.

### 4.1. Isotopy and Gauge Transformation Symmetries

The HyperCube model admits fundamental symmetries that we leverage for analysis.

**Gauge Freedom.** The HyperCube product  $T(\cdot)$  is *invariant* under the continuous group of invertible *gauge transformations*: For any invertible  $U, V, W \in \mathrm{GL}(n, \mathbb{C})$ , the transformation

$$\Theta' = (A', B', C'), \quad A'_a = UA_aV^{-1}, \quad B'_b = VB_bW^{-1}, \quad C'_c = WC_cU^{-1} \quad (9)$$

preserves the product:  $T_{abc}(\Theta') = \frac{1}{n} \mathrm{Tr}(A'_a B'_b C'_c) = T_{abc}(\Theta)$ . However, the objective function  $\mathcal{H}$  contains Frobenius norms, which restricts the symmetry of the *optimization landscape* to the unitary subgroup  $\mathrm{U}(n)$  (where  $U, V, W$  are unitary).

**Isotopy Equivariance.** The product is *equivariant* under *permutations* of the factor's index sets: For any bijections  $(\phi, \psi, \chi)$ ,  $T_{abc}(\Theta') = T_{\phi(a)\psi(b)\chi(c)}(\Theta)$ , where  $\Theta' = (A_{\phi(a)}, B_{\psi(b)}, C_{\chi(c)})$ .

### 4.2. Unitary Collinear Factorization $\iff$ Group Isotope

Here, we establish a fundamental equivalence: a finite quasigroup admits a **unitary collinear factorization** *if and only if* it is isotopic to a group. We prove that this algebraic structure is both necessary (Theorem 7) and sufficient (Lemma 8), and that the factorization itself is *unique*: it is unitarily equivalent to the left-regular representation of the underlying group.

**Reduction to Loops.** Every finite quasigroup  $(Q, \circ)$  is isotopic to a loop  $(Q, \circ')$ —a quasigroup with identity  $e$  (Pflugfelder, 1990). Since  $T(\cdot)$  is equivariant under isotopy, the existence of a unitary collinear factorization for  $(Q, \circ)$  implies the existence of one for the loop  $(Q, \circ')$ . Thus, without loss of generality, we establish the following results for the class of loops.

**Lemma 5 (Synchronization)** *Let  $(Q, \circ')$  be a finite loop admitting a unitary collinear factorization  $\Theta$ . There exists a unitary gauge  $(U, V, W)$  such that the transformed slices satisfy the synchronized condition:*

$$A'_g = B'_g = (C'_g)^\dagger =: \rho(g), \quad \forall g \in Q. \quad (10)$$

**Proof [Sketch]** We explicitly define the gauge  $(U, V, W) := (A_e^\dagger, I_n, B_e)$ . By exploiting the loop identity properties ( $g \circ' e = e \circ' g = g$ ) within the collinearity constraint  $A_a B_b = C_c^\dagger$ , one can derive  $A_g B_e = A_e B_g$ . Substituting this relation into the gauge definition directly verifies the synchronization condition  $A'_g = B'_g = (C'_g)^\dagger$ . (See Appendix D.)  $\blacksquare$

**Lemma 6 (Homomorphism & Injectivity)** *Under the synchronizing gauge of Lemma 5, the map  $\rho : Q \rightarrow U(n)$  is an injective homomorphism. Specifically:*

$$\rho(a)\rho(b) = \rho(a \circ b) \quad \forall a, b \in Q, \quad \text{and} \quad \rho(x) \neq \rho(y) \quad \text{for } x \neq y.$$

**Proof (Homomorphism)** For any supported triple  $(a, b, c)$ , the collinear identities (7) imply  $A_a B_b = T_{abc} C_c^\dagger / \|C_c\|^2$ . Since  $\|C_c\|^2 = 1$  (unitarity) and  $T_{abc} = 1$  on the support (from  $T = \delta$ ), this enforces the strict equality  $A'_a B'_b = (C'_c)^\dagger$ . In the synchronizing gauge, this reduces to  $\rho(a)\rho(b) = \rho(c) = \rho(a \circ b)$ . *(Injectivity)* For any distinct  $x, y \in Q$ , the corresponding target slices are distinct ( $\delta_{x::} \neq \delta_{y::}$ ), because a Latin square has no duplicate rows. Since the feasible model ( $T = \delta$ ) reconstructs these slices via  $T_{xbc} = \langle \rho(x)^\dagger, \rho(b)\rho(c)^\dagger \rangle$ ,  $\rho(x)$  and  $\rho(y)$  must be distinct. ■

**Theorem 7 (Unitary Collinearity  $\implies$  Group Isotope)** *Let  $(Q, \circ)$  be a finite quasigroup admitting a unitary collinear factorization. Then,  $(Q, \circ)$  is isotopic to a group.*

**Proof** As established in the reduction, if  $(Q, \circ)$  admits a unitary collinear factorization, so does its loop isotope  $(Q, \circ')$ . By Lemma 5, this factorization induces a synchronized map  $\rho : Q \rightarrow U(n)$ . Since  $\rho$  is a homomorphism (Lemma 6), invoking associativity of matrix multiplication yield:

$$\rho((x \circ' y) \circ' z) = \rho(x)\rho(y)\rho(z) = \rho(x \circ' (y \circ' z)).$$

Since  $\rho$  is injective (Lemma 6), this equality implies associativity of  $\circ'$ :  $(x \circ' y) \circ' z = x \circ' (y \circ' z)$ . Thus, the loop  $(Q, \circ')$  is a group, and the original quasigroup  $(Q, \circ)$  is a group isotope. ■

**Lemma 8 (Unitary Collinearity  $\Leftarrow$  Group Isotope)** *Conversely, every group isotope admits a unitary collinear factorization.*

**Proof** Let  $(Q, \circ)$  be isotopic to a group  $(Q, \circ')$ . The left-regular representation  $\rho$  of the group defines a unitary collinear factorization via  $A_g = B_g = C_g^\dagger = \rho(g)$  (satisfying  $T = \delta$  and  $\mathcal{R} = 0$ ). By isotopy equivariance of  $T(\cdot)$ , this induces a valid unitary collinear factorization for  $(Q, \circ)$ . ■

**Lemma 9 (Uniqueness of Representation)** *Let  $(Q, \circ')$  be the group identified in Theorem 7. The induced map  $\rho : Q \rightarrow U(n)$  is unitarily equivalent to the left-regular representation of  $(Q, \circ')$ .*

**Proof** Since  $\rho$  is a homomorphism, the feasibility constraint on the triple  $(g, e, e)$  implies  $T_{gee} = \frac{1}{n} \text{Tr}(\rho(g)\rho(e)\rho(e)^\dagger) = \frac{1}{n} \text{Tr}(\rho(g \circ' e \circ' e^{-1})) = \frac{1}{n} \text{Tr}(\rho(g)) = \delta_{gee}$ . Thus, the character of  $\rho$  is  $\text{Tr}(\rho(g)) = n \cdot \delta_{gee} = n \cdot \mathbb{I}_{\{g=e\}}$ , which is exactly the character of the left-regular representation. By character theory, this uniquely determines the representation up to unitary equivalence. ■

**Remark.** Theorem 7 and Lemma 8 establish a precise bidirectional correspondence: a quasigroup admits a unitary collinear factorization *if and only if* it is a group isotope. Lemma 9 shows that all such unitary factorizations are equivalent up to unitary gauge transformations. Theorem 12 (Section 5) generalizes these results to general (non-unitary) collinear factorizations.

## 5. Spectral Geometry of Collinear Manifold

In this section, we broaden our analysis of the collinear manifold by relaxing the feasibility and unitarity constraints. This reveals that geometric alignment alone dictates the factors' **spectral structure** via rigid projection identities, enabling us to extend the fundamental equivalence of Section 4 to the non-unitary setting (Theorem 12). Furthermore, we characterize  $\mathcal{H}$  as a **rank-maximizing potential** promoting global norm balance, and uniquely identify its global optimum within this manifold.

**Lemma 10 (Shared Gram Matrices)** *Assume perfect collinearity  $\mathcal{R}(\Theta) = 0$  and  $|T_{abc}| > 0$  on the support. There exist index-independent, trace- $n$  PSD Gram matrices  $X, Y, Z$  such that:*

$$X = \frac{A_a A_a^\dagger}{\|A_a\|^2} = \frac{C_c^\dagger C_c}{\|C_c\|^2}, \quad Y = \frac{B_b B_b^\dagger}{\|B_b\|^2} = \frac{A_a^\dagger A_a}{\|A_a\|^2}, \quad Z = \frac{C_c C_c^\dagger}{\|C_c\|^2} = \frac{B_b^\dagger B_b}{\|B_b\|^2}. \quad (11)$$

**Proof** Fix a supported triple  $(a, b, c)$ . From the identities in (8), we have:

$$\frac{T_{abc}}{\|A_a\|^2} A_a A_a^\dagger = A_a (B_b C_c) = (A_a B_b) C_c = \frac{T_{abc}}{\|C_c\|^2} C_c^\dagger C_c.$$

Cancelling the nonzero scalar  $T_{abc}$ , one obtains  $A_a A_a^\dagger / \|A_a\|^2 = C_c^\dagger C_c / \|C_c\|^2$ . The Latin-square property ensures that for any fixed  $a$ , as we vary  $b$ , the index  $c$  varies uniquely to maintain support. The left side depends only on  $a$ , while the right side depends only on  $c$ . Since the support graph of a quasigroup is connected, this equality propagates across all indices, implying both sides equal a constant matrix  $X$ . Taking the trace yields  $\text{Tr}(X) = \text{Tr}(A_a A_a^\dagger) / \|A_a\|^2 = n \|A_a\|^2 / \|A_a\|^2 = n$ . The remaining equalities for  $Y$  and  $Z$  are obtained analogously.  $\blacksquare$

**Lemma 11 (Normalized Rank  $\kappa$ )** *Assume perfect collinearity  $\mathcal{R}(\Theta) = 0$ . For any supported triple  $(a, b, c)$ , the dimensionless ratio*

$$\kappa_{abc} := \frac{\|A_a\|^2 \|B_b\|^2 \|C_c\|^2}{|T_{abc}|^2}$$

*is constant across the support; denote this value by  $\kappa$ . This constant enforces the projection identity  $X = \kappa X^2$  (similarly for  $Y, Z$ ), identifying  $\kappa$  as the normalized rank:*

$$\kappa = \frac{\text{rank}(X)}{n} \leq 1, \quad (12)$$

*with equality ( $\kappa = 1$ ) if and only if the Gram matrices are full-rank ( $X = Y = Z = I_n$ ).*

**Proof** Substituting the alignment identities (8) into the Gram definition yields the relation  $X = \kappa_{abc} X^2$  for any supported triple  $(a, b, c)$  (derivation in Appendix D). Since  $X$  is index-independent, the coefficient  $\kappa_{abc}$  must be a constant  $\kappa$ . Define  $P := \kappa X$ . Then  $P^2 = \kappa^2 X^2 = \kappa X = P$ , making  $P$  an orthogonal projection. Thus,  $\text{rank}(X) = \text{rank}(P) = \text{Tr}(P) = \kappa \text{Tr}(X) = \kappa n$ . Rearranging yields  $\kappa = \text{rank}(X)/n \leq 1$ . If  $\kappa = 1$ , then  $X$  is a trace- $n$  projection, implying  $X = I_n$ .  $\blacksquare$

**Theorem 12 (Collinearity-Associativity Equivalence)** *Let  $(Q, \circ)$  be a finite quasigroup. The feasible collinear manifold is non-empty if and only if  $(Q, \circ)$  is isotopic to a group.*

**Proof [Sketch]** The proof leverages the spectral rigidity established in Section 5. Specifically, the projection identities of Lemma 11 (e.g.,  $X = \kappa X^2$ ) restrict the factor slices to be *scaled isometries* on their active subspaces (e.g.,  $A_a A_a^\dagger \propto I_{\text{Range}(X)}$ ). This rigid geometric condition admits a unitary gauge transformation that synchronizes the factor slices (analogous to Lemma 5), recovering a *projective representation* of a group. (See Appendix E for the full proof.)  $\blacksquare$

### 5.1. Restricted Optimality on Collinear Manifold

Leveraging the spectral rigidity established above, we now uniquely identify the global optimum of the objective (4) restricted to the collinear manifold.

**Lemma 13 (AM–GM Lower Bound)** *Assume perfect collinearity  $\mathcal{R}(\Theta) = 0$ . The objective  $\mathcal{H}$  satisfies the absolute lower bound:*

$$\mathcal{H}(\Theta) = \mathcal{B}(\Theta; \delta) \geq 3 \sum_{a,b,c} \delta_{abc} |T_{abc}|^{4/3}. \quad (13)$$

*Equality holds if and only if the normalized rank is maximal ( $\kappa = 1$ ) and the factor slice norms are strictly balanced ( $\|A_a\|^2 = \|B_b\|^2 = \|C_c\|^2$  for all indices).*

**Proof** Let  $\alpha_a := \|A_a\|^{-2}$ ,  $\beta_b := \|B_b\|^{-2}$ , and  $\gamma_c := \|C_c\|^{-2}$ . Note that  $\alpha_a \beta_b \gamma_c = \kappa^{-1} |T_{abc}|^{-2}$ . Applying the AM–GM inequality ( $\alpha + \beta + \gamma \geq 3(\alpha\beta\gamma)^{1/3}$ ) to the definition of  $\mathcal{B}$  yields:

$$\mathcal{B}(\Theta; \delta) = \sum_{a,b,c} \delta_{abc} |T_{abc}|^2 (\alpha_a + \beta_b + \gamma_c) \geq 3\kappa^{-1/3} \sum_{a,b,c} \delta_{abc} |T_{abc}|^{4/3}. \quad (14)$$

Since  $\kappa \leq 1$  (Lemma 11), the factor  $\kappa^{-1/3}$  is minimized at the boundary  $\kappa = 1$ , establishing the absolute lower bound (13). Equality in (13) holds if and only if  $\kappa = 1$  and the AM–GM equality condition  $\alpha_a = \beta_b = \gamma_c$  is satisfied for every supported triple  $(a, b, c)$ . Due to the connectivity of the quasigroup support graph (Appendix C), these local equalities propagate globally, ensuring all factor norms are equal:  $\|A_a\|^2 = \|B_b\|^2 = \|C_c\|^2$ . ■

**Remark.** Lemma 13 reveals that  $\mathcal{B}$  effectively balances the (inverse) factor slice norms. Once the norms balanced, (14) decomposes into a *scale-free* term  $\kappa^{-1/3}$  that penalizes rank deficiency, and a term that depends *solely* on the model’s output  $T$ . Consequently, when  $T$  is fixed (*i.e.*, feasibility  $T = \delta$ ), the objective acts purely as a rank-maximizing potential on the collinear manifold.

**Theorem 14 (Optimality within Collinear Manifold)** *Let  $(Q, \circ)$  be a finite quasigroup admitting a collinear factorization (*i.e.*, a group isotope, per Theorem 12). Restricted to the feasible collinear manifold  $\mathcal{F}_\delta \cap \{\Theta \mid \mathcal{R}(\Theta; \delta) = 0\}$ , the minimum of  $\mathcal{H}$  is achieved by a **unitary** collinear factorization (unique up to unitary gauge symmetry), and the minimum value is  $3 |\delta|$ .*

**Proof** For feasible points (where  $|T_{abc}| = 1$ ), Lemma 13 implies the absolute lower bound:

$$\mathcal{H}(\Theta) \geq 3 \sum_{a,b,c} \delta_{abc} |T_{abc}|^{4/3} = 3 |\delta|.$$

Attaining this minimum requires satisfying two conditions simultaneously: maximal rank ( $\kappa = 1$ ) and globally balanced factor norms ( $\|A_a\|^2 = \|B_b\|^2 = \|C_c\|^2$  for all indices). The definition  $\kappa = \|A_a\|^2 \|B_b\|^2 \|C_c\|^2 / |T_{abc}|^2$  (from Lemma 11) combined with  $\kappa = 1$  and  $|T_{abc}| = 1$  uniquely determines this common norm as 1. Finally, since  $\kappa = 1$ , the shared Gram matrices are identity matrices (Lemma 11). Combined with the unit norm condition ( $A_a A_a^\dagger = \|A_a\|^2 X = I_n$ ), this confirms the factorization is strictly unitary. Existence is guaranteed by Lemma 8, and uniqueness is guaranteed by Lemma 9, respectively. ■

## 6. Global Landscape and the Dominance Mechanism

We now address the optimization problem over the full feasible set  $\mathcal{F}_\delta := \{\Theta \mid T(\Theta) = \delta\}$ :

$$\mathcal{H}_{\min}(\delta) := \inf_{\Theta \in \mathcal{F}_\delta} \mathcal{H}(\Theta). \quad (15)$$

Through this analysis, we aim to resolve the two fundamental challenges posed in Section 1: (1) characterizing the optimal parameters  $\Theta^*$  for a given target  $\delta$  (explaining the bias toward unitary collinear factorizations), and (2) comparing the minimum objective values  $\mathcal{H}_{\min}(\delta)$  across different algebraic structures (explaining the bias toward group isotopes).

**Analytical Strategy.** To rigorously characterize the global minimizers, we decompose the analysis along two strategic axes: the geometric domain (collinear manifold vs. global landscape) and the algebraic target (group isotopes vs. general quasigroups). We first isolate the *collinear manifold* ( $\mathcal{R} = 0$ ) and solve for the exact minimizers in this tractable domain (Section 5.1). We then bridge this restricted analysis to the global landscape via a **dominance argument**, positing that the steep misalignment penalty  $\mathcal{R}$  precludes escape from this manifold. This allows us to prove global optimality for group isotopes (Section 6.2) and establish a strict optimality gap for non-group structures (Section 6.3).

### 6.1. Feasibility and Existence Framework

We first establish a rigorous optimization framework. While the unregularized problem admits non-compact gauge symmetries that complicate a direct existence proof, we prove that the problem is well-posed under Tikhonov regularization and analyze the consistency of the vanishing-regularization limit.

**Lemma 15 (Feasibility)** *For any binary third-order tensor  $\delta \in \{0, 1\}^{n \times n \times n}$ , there exists a finite-norm parameter triple  $\Theta = (A, B, C)$  such that  $T(\Theta) = \delta$ . Consequently, for any Cayley tensor  $\delta$  of a finite quasigroup, the feasible set  $\mathcal{F}_\delta$  is nonempty.*

**Proof [Sketch]** Proof by explicit construction (see Appendix D). ■

Existence of minimizers for the unregularized problem is subtle due to non-compact gauge symmetries. To ensure rigor, we first establish existence for a Tikhonov-regularized objective and then consider the vanishing-regularization limit.

**Theorem 16 (Regularized Existence)** *For any  $\epsilon > 0$  and target  $\delta$ , define the regularized objective  $\mathcal{H}_\epsilon(\Theta) := \mathcal{H}(\Theta) + \epsilon \|\Theta\|_F^2$ . Then,  $\min_{\Theta \in \mathcal{F}_\delta} \mathcal{H}_\epsilon(\Theta)$  admits a global minimizer  $\Theta_\epsilon^* \in \mathcal{F}_\delta$ .*

**Proof [Sketch]** The regularized objective is continuous and coercive, and the feasible set is closed and nonempty (Lemma 15). Existence follows from the Weierstrass Extreme Value Theorem. (See Appendix D.) ■

**Corollary 17 (Consistency limit)** *Let  $\epsilon_k \rightarrow 0$  and let  $\Theta_{\epsilon_k}^*$  be global minimizers of  $\mathcal{H}_{\epsilon_k}$  over  $\mathcal{F}_\delta$ . If the sequence  $\{\Theta_{\epsilon_k}^*\}$  admits an accumulation point  $\Theta^*$ , then  $\Theta^*$  is a global minimizer of the unregularized objective  $\mathcal{H}$  over  $\mathcal{F}_\delta$ .*

**Proof [Sketch]** Follows from the continuity of  $\mathcal{H}$  and the limit of the optimality inequality  $\mathcal{H}_{\epsilon_k}(\Theta_{\epsilon_k}^*) \leq \mathcal{H}_{\epsilon_k}(\Theta')$ . (See Appendix D.) ■

**Remark on Unregularized Existence.** While Corollary 17 is conditional, we note that extensive experiments consistently show parameter stabilization. In Appendix F, we discuss the geometric obstructions to a direct existence proof (specifically non-compact gauge orbits) and provide a theoretical mechanism—gauge fixing via balanced representations—that controls these directions.

## 6.2. The Ideal Case: Optimality for Group Isotopes

We begin with the class of **group isotopes**. This represents the *ideal* case where the feasible collinear manifold is non-empty, allowing us to anchor the global analysis in the rigid spectral geometry of  $\mathcal{B}$ .

Theorem 14 establishes the unique structural optimum of the objective within the collinear manifold. To assert global optimality, we must theoretically preclude the existence of spurious non-collinear basins ( $\mathcal{R} > 0$ ) where a reduction in the base term  $\mathcal{B}$  might outweigh the incurred alignment error  $\mathcal{R}$ . Empirically, however, we observe that such a trade-off is never favorable; optimization trajectories consistently converge to the collinear set, suggesting that  $\mathcal{R}$  functions as a globally dominant penalty. We formalize this observation as follows:

**Conjecture 18 (Weak Collinearity Dominance)** *Let  $\delta$  be the Cayley tensor of a finite group isotope (implying the feasible collinear set  $\{\Theta \in \mathcal{F}_\delta \mid \mathcal{R}(\Theta; \delta) = 0\}$  is non-empty). Then, every global minimizer of the unregularized objective (15) lies on the collinear manifold.*

**Theorem 19 (Global Optimality for Group Isotopes)** *Let  $\delta$  correspond to a finite group isotope. Assume Conjecture 18 holds and that the infimum in (15) is attained. Then, every global minimizer of (15) is a **unitary collinear** factorization, achieving*

$$\mathcal{H}_{\min}(\delta) = 3 |\delta|.$$

**Proof** By Conjecture 18, any global minimizer must satisfy  $\mathcal{R} = 0$ . Consequently, the problem reduces to minimizing  $\mathcal{B}$  on the feasible collinear manifold. By Theorem 14, the minimum on this manifold is attained exclusively by unitary factorizations with value  $3 |\delta|$ .  $\blacksquare$

**Remark.** While empirical stability is robust, formally verifying the Hessian spectrum at  $\Theta^*$  faces intrinsic geometric hurdles due to gauge singularities and the graph-theoretic nature of the tangent space. We detail these specific obstructions and their link to the **coefficient graph Laplacian** in Appendix F.2.3.

## 6.3. The General Case: Optimality for Non-Group Isotopes

We finally address the setting of general quasigroups. Specifically, consider a target  $\delta$  that is not a group isotope. By Theorem 12, the collinear manifold for such a target is empty, necessitating a strictly positive misalignment penalty ( $\mathcal{R} > 0$ ). This structural obstruction forces a direct variational conflict: the optimizer must balance the drive for spectral regularity ( $\mathcal{B}$ ) against the unavoidable alignment error ( $\mathcal{R}$ ). To characterize the inductive bias in this general setting, we propose that the landscape is governed by a strict **variational hierarchy** where the misalignment cost  $\mathcal{R}$  outweighs potential reductions in  $\mathcal{B}$ .

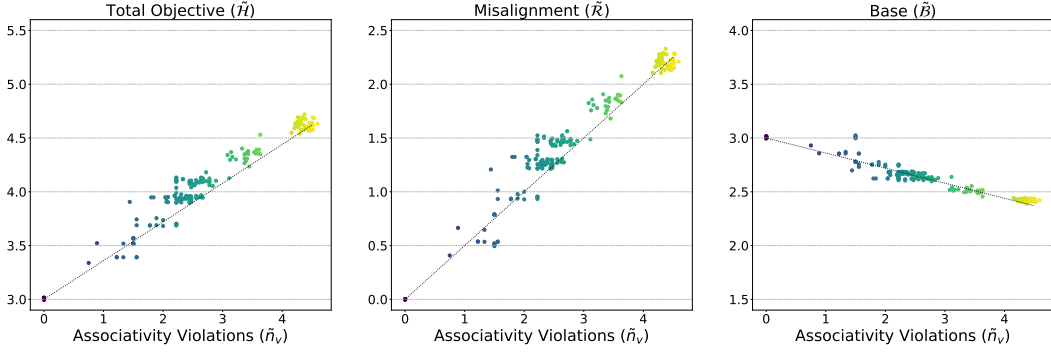


Figure 1: Empirical verification of Strong Collinearity Dominance. Scatter plots showing the normalized objective terms ( $\tilde{\mathcal{H}}$ ,  $\tilde{\mathcal{R}}$ ,  $\tilde{\mathcal{B}}$ ) versus the normalized associativity violation  $\tilde{n}_v$  for reduced Latin squares corresponding to loops. (Middle) The misalignment penalty  $\tilde{\mathcal{R}}$  grows linearly with non-associativity ( $c_R \approx 0.50$ ). (Right)  $\tilde{\mathcal{B}}$  decreases linearly ( $c_B \approx 0.14$ ), confirming the variational trade-off. (Left) The total objective  $\tilde{\mathcal{H}}$  exhibits a net positive slope ( $c_H \approx 0.36$ ), confirming that the misalignment penalty dominates the trade-off, forcing the global minimum to the group structure ( $\tilde{n}_v = 0$ ). (See Appendix B.)

**Conjecture 20 (Strong Collinearity Dominance)** *For any quasigroup target  $\delta$ , the misalignment penalty  $\mathcal{R}$  dominates  $\mathcal{B}$  across the global feasible landscape. A sufficient quantitative realization of this dominance can be formalized by the inequality such that for all  $\Theta \in \mathcal{F}_\delta$ :*

$$\mathcal{B}(\Theta; \delta) \geq 3|\delta| - c\mathcal{R}(\Theta; \delta), \quad c \in [0, 1]. \quad (16)$$

Under this condition, the objective satisfies  $\mathcal{H} = \mathcal{B} + \mathcal{R} \geq 3|\delta| + (1 - c)\mathcal{R}$ . Since  $c < 1$ , any non-collinear solution ( $\mathcal{R} > 0$ ) strictly increases the total cost.

**Remark.** We distinguish these conjectures to decouple the *result* from the *mechanism*. Conjecture 18 (Weak) posits the result: for group isotopes, the global minimizer is collinear. Conjecture 20 (Strong) identifies the mechanism: the misalignment penalty  $\mathcal{R}$  dominates  $\mathcal{B}$ . While Strong Dominance implies the Weak form, it offers a broader landscape characterization valid even in the non-group setting.

**Theorem 21 (Strict Gap for Non-Group Isotopes)** *Assume Conjecture 20 holds and that the infimum in (15) is attained. Then:*

$$\mathcal{H}_{\min}(\delta) \geq 3|\delta|, \quad (17)$$

*with equality if and only if  $\delta$  is isotopic to a group. Consequently, among all quasigroups of fixed order  $n$ , group isotopes uniquely achieve the minimal objective value.*

**Proof (Sufficiency)** If  $\delta$  is a group isotope, Lemma 8 guarantees a unitary solution where  $\mathcal{H} = 3|\delta|$ . (Necessity) If  $\delta$  is not a group isotope, Theorem 12 implies  $\mathcal{R}(\Theta^*) > 0$  for any feasible point. Conjecture 20 then yields  $\mathcal{H}_{\min}(\delta) \geq 3|\delta| + (1 - c)\mathcal{R}(\Theta^*) > 3|\delta|$ . [Need coercivity for complete proof?]  $\blacksquare$

**Empirical Verification** We empirically investigated Conjecture 20 by analyzing the converged minima across diverse Latin square targets  $\delta$ . As illustrated in Figure 1, we observe a striking linear scaling law between the objective terms and the (normalized) associativity violation  $\tilde{n}_v$ . Specifically, the misalignment penalty  $\mathcal{R}$  scales significantly faster ( $c_R \approx 0.50$ ) than the corresponding reduction in  $\mathcal{B}$  ( $c_B \approx 0.14$ ). This yields an **effective trade-off rate** of  $c = c_B/c_R \approx 0.28 < 1$ . While this fit represents an average behavior, the substantial margin below the critical threshold provides robust evidence for the strict dominance inequality postulated in Conjecture 20. Consequently,  $\mathcal{H}_{\min}$  consistently tracks  $\tilde{n}_v$ , validating its utility as a differentiable, isotopy-invariant proxy for group structure. (See Appendix B for full details.)

## 7. Conclusion and Future Work

This work provides a rigorous theoretical foundation for the HyperCube architecture, establishing it as a differentiable proxy for algebraic associativity. By isolating the **collinear manifold**, we uncovered an **intrinsic geometric-algebraic equivalence**: the architecture mediates a rigid correspondence where factor alignment necessitates group structure. Within this manifold, we proved that the objective functions as a **rank-maximizing potential**, unconditionally driving the representation toward full-rank, unitary configurations. Globally, we proposed a **variational hierarchy** where the cost of misalignment ( $\mathcal{R}$ ) dominates spectral reduction ( $\mathcal{B}$ ), ensuring that global minima are sequestered within the regime of perfect group isotopes.

**The Geometry of Unitarity Bias.** Our results highlight a fundamental departure from the *Low-Rank Simplicity Bias* prevalent in modern learning theory. While standard models generalize via parsimonious compression, HyperCube’s structural bias promotes **unitarity and rank maximization**. This mirrors the geometry of the Group Fourier Transform, where full rank is required to span the complete spectral basis and unitarity ensures energy conservation (Parseval’s identity). This suggests that for algebraic discovery, the path to systematic generalization lies in the rigid, energy-preserving constraints of unitary representations.

**Open Analytical Challenges.** The primary theoretical hurdle remains a formal proof of the *Strong Collinearity Dominance Conjecture*. While our results establish the optimality of the collinear manifold *internally*, proving its global dominance requires showing that the misalignment penalty  $\mathcal{R}$  always outweighs the potential spectral reduction of  $\mathcal{B}$  for group and non-group targets. Furthermore, a local stability analysis of the Hessian at  $\Theta^*$  remains extremely difficult. This complexity arises not only from the high-order polynomial interaction between the quartic loss and trilinear constraints, but also from the non-compact gauge orbits inherent to tensor factorizations. While we have identified the **coefficient graph Laplacian** as a key structural element of the tangent space, a full characterization of the landscape’s coercivity remains a deep open question.

**Future Directions.** We aim to integrate this algebraic discovery mechanism into neural architectures operating on raw data, enabling models to discover *invariant causal laws* rather than mere statistical artifacts. By shifting from manual symmetry prescription to automated structural discovery, we move toward architectures that can distinguish universal principles from spurious correlations through the lens of latent algebraic symmetry.

## References

Sanjeev Arora, Nadav Cohen, Wei Hu, and Yuping Luo. Implicit Regularization in Deep Matrix Factorization, October 2019. URL <http://arxiv.org/abs/1905.13655>. arXiv:1905.13655 [cs, stat].

Michael M. Bronstein, Joan Bruna, Taco Cohen, and Petar Veličković. Geometric Deep Learning: Grids, Groups, Graphs, Geodesics, and Gauges, May 2021. URL <http://arxiv.org/abs/2104.13478>. arXiv:2104.13478 [cs, stat].

Emmanuel J. Candes and Terence Tao. The Power of Convex Relaxation: Near-Optimal Matrix Completion. *IEEE Transactions on Information Theory*, 56(5):2053–2080, May 2010. ISSN 0018-9448, 1557-9654. doi: 10.1109/TIT.2010.2044061. URL <http://ieeexplore.ieee.org/document/5452187/>.

Emmanuel J. Candès and Benjamin Recht. Exact Matrix Completion via Convex Optimization. *Foundations of Computational Mathematics*, 9(6):717–772, December 2009. ISSN 1615-3383. doi: 10.1007/s10208-009-9045-5. URL <https://doi.org/10.1007/s10208-009-9045-5>.

Taco Cohen and Max Welling. Group Equivariant Convolutional Networks. In *Proceedings of The 33rd International Conference on Machine Learning*, pages 2990–2999. PMLR, June 2016. URL <https://proceedings.mlr.press/v48/cohenc16.html>. ISSN: 1938-7228.

M. Fazel, H. Hindi, and S.P. Boyd. A rank minimization heuristic with application to minimum order system approximation. In *Proceedings of the 2001 American Control Conference. (Cat. No.01CH37148)*, volume 6, pages 4734–4739 vol.6, June 2001. doi: 10.1109/ACC.2001.945730. URL <https://ieeexplore.ieee.org/document/945730>. ISSN: 0743-1619.

Robert Geirhos, Jörn-Henrik Jacobsen, Claudio Michaelis, Richard Zemel, Wieland Brendel, Matthias Bethge, and Felix A Wichmann. Shortcut learning in deep neural networks. *Nature Machine Intelligence*, 2(11):665–673, 2020.

David J Gross. The role of symmetry in fundamental physics. *Proceedings of the National Academy of Sciences*, 93(25):14256–14259, 1996.

Suriya Gunasekar, Blake E Woodworth, Srinadh Bhojanapalli, Behnam Neyshabur, and Nati Srebro. Implicit Regularization in Matrix Factorization. In *Advances in Neural Information Processing Systems*, volume 30. Curran Associates, Inc., 2017. URL <https://papers.nips.cc/paper/2017/hash/58191d2a914c6dae66371c9dc91b41-Abstract.html>.

Dongsung Huh. Discovering group structures via unitary representation learning. In *The Thirteenth International Conference on Learning Representations*, 2025. URL <https://openreview.net/forum?id=Tz8Li6G2xU&noteId=Tz8Li6G2xU>.

Minyoung Huh, Hossein Mobahi, Richard Zhang, Brian Cheung, Pulkit Agrawal, and Phillip Isola. The Low-Rank Simplicity Bias in Deep Networks, March 2023. URL <http://arxiv.org/abs/2103.10427>. arXiv:2103.10427 [cs].

Arthur Jacot. Implicit Bias of Large Depth Networks: a Notion of Rank for Nonlinear Functions. September 2022. URL <https://openreview.net/forum?id=6iDHce-0B-a>.

Brenden Lake and Marco Baroni. Generalization without systematicity: On the compositional skills of sequence-to-sequence recurrent networks. In *International conference on machine learning*, pages 2873–2882. PMLR, 2018.

Emmy Noether. Invariante variationsprobleme. In *Gesammelte Abhandlungen-Collected Papers*, pages 231–239. Springer, 1918.

Hala O Pflugfelder. *Quasigroups and Loops: Introduction*, volume 7 of *Sigma Series in Pure Mathematics*. Heldermann Verlag, Berlin, 1990.

Alethea Power, Yuri Burda, Harri Edwards, Igor Babuschkin, and Vedant Misra. Grokking: Generalization Beyond Overfitting on Small Algorithmic Datasets, January 2022.

Noam Razin, Asaf Maman, and Nadav Cohen. Implicit Regularization in Tensor Factorization. In *Proceedings of the 38th International Conference on Machine Learning*, pages 8913–8924. PMLR, July 2021. URL <https://proceedings.mlr.press/v139/razin21a.html>. ISSN: 2640-3498.

Andrew M. Saxe, James L. McClelland, and Surya Ganguli. Exact solutions to the nonlinear dynamics of learning in deep linear neural networks, February 2014. URL <http://arxiv.org/abs/1312.6120>. arXiv:1312.6120 [cond-mat, q-bio, stat].

Ashish Vaswani, Noam Shazeer, Niki Parmar, Jakob Uszkoreit, Llion Jones, Aidan N Gomez, Łukasz Kaiser, and Illia Polosukhin. Attention is all you need. *Advances in neural information processing systems*, 30, 2017.

Eugene Paul Wigner. *Symmetries and Reflections. Scientific Essays of Eugene P. Wigner*. Indiana University Press, 1967.

## Appendix A. Enumeration and Symmetry Classes

While the main text formulates the problem for general quasigroups, our experimental analysis (Section 6.3) relies on the enumeration of loops to track the search space size.

**Loops and Reduced Latin Squares.** A loop is a quasigroup with a two-sided identity element  $e \in Q$ . If we label the elements of  $Q$  as  $\{0, 1, \dots, n - 1\}$  with  $0 = e$ , the operation table is a *reduced* (or normalized) Latin square, where the first row and first column are in natural order  $(0, 1, \dots, n - 1)$ . Classifying loops of order  $n$  is equivalent to classifying reduced Latin squares of order  $n$ .

**Isomorphism vs. Isotopy.** The enumeration of distinct structures depends on the chosen notion of equivalence:

- **Loop Isomorphism (Simultaneous Relabeling):** Two loops are isomorphic if they differ by a bijection  $\phi : Q \rightarrow Q'$  satisfying  $\phi(a) \circ' \phi(b) = \phi(a \circ b)$ . In terms of Latin squares, this corresponds to applying the *same* permutation to rows, columns, and symbol labels simultaneously. We use this relation to identify unique loops.
- **Quasigroup Isotopy (Independent Relabeling):** The HyperCube model, which treats the operation as a 3-way tensor without a privileged identity, naturally respects a larger internal symmetry group. Two Latin squares are *isotopic* if they differ by an arbitrary triple of permutations  $(\phi, \psi, \chi) \in S_n \times S_n \times S_n$  acting independently on rows, columns, and symbols.

Since the HyperCube objective is invariant under this larger group, counting distinct structures for the model corresponds to counting quasigroup isotopy classes (orbits of  $S_n^3$ ).

## Appendix B. Empirical Verification

**Objective.** We empirically investigate the **Strong Collinearity Dominance Conjecture** (Conjecture 20). Specifically, we aim to quantify the variational trade-off between the misalignment penalty  $\mathcal{R}$  and the base term  $\mathcal{B}$ . Recall that the conjecture posits a bound  $\mathcal{B} \geq 3|\delta| - c\mathcal{R}$  with  $c < 1$ , implying that the savings in  $\mathcal{B}$  are outweighed by the penalty in  $\mathcal{R}$ .

**Experimental Setup.** We analyze reduced Latin squares  $\delta$  corresponding to loops of orders  $n \in \{5, 6, 7, 8\}$ . For the smaller orders  $n \in \{5, 6\}$ , we exhaustively evaluate all unique loops up to isomorphism (6 and 106 cases, respectively). For  $n \in \{7, 8\}$ , we evaluate a random subset of 100 loops per order, due to the combinatorial explosion of the search space (e.g., 23,746 unique loops for  $n = 7$ ). For each  $\delta$ , we compute the global minimum  $\mathcal{H}_{\min}(\delta)$  using a gradient-based optimizer with multiple random initial values to mitigate local minima. To correlate the landscape geometry with algebraic structure, we measure the normalized associativity violations:

$$\tilde{n}_v(\delta) := \frac{1}{|\delta|} \sum_{a,b,c} \mathbb{I}_{\{(a \circ b) \circ c \neq a \circ (b \circ c)\}}.$$

Note that  $\tilde{n}_v = 0$  if and only if  $\delta$  encodes a group.

**Results.** We analyze the normalized objective terms ( $\tilde{\mathcal{R}} := \mathcal{R}_{\min}/|\delta|$ ,  $\tilde{\mathcal{B}} := \mathcal{B}_{\min}/|\delta|$ ,  $\tilde{\mathcal{H}} := \mathcal{H}_{\min}/|\delta|$ ) as a function of the violation metric  $\tilde{n}_v$ . The data reveals a striking linear scaling law across the space of Latin squares:

$$\begin{aligned}\tilde{\mathcal{R}}(\delta) &\approx c_R \cdot \tilde{n}_v(\delta) & (c_R \approx 0.50) \\ \tilde{\mathcal{B}}(\delta) &\approx 3 - c_B \cdot \tilde{n}_v(\delta) & (c_B \approx 0.14) \\ \tilde{\mathcal{H}}(\delta) &\approx 3 + c_H \cdot \tilde{n}_v(\delta) & (c_H = c_R - c_B \approx 0.36).\end{aligned}\quad (18)$$

**Confirmation of Dominance.** These affine relations provide precise quantitative verification of the *Strong Collinearity Dominance Conjecture* (Conjecture 20). We identify the constant  $c$  in the conjectured bound  $\mathcal{B} \geq 3|\delta| - c\mathcal{R}$  as the ratio of the empirical slopes:

$$c \approx \frac{c_B}{c_R} \approx \frac{0.14}{0.50} = 0.28.$$

Since  $c \approx 0.28 < 1$ , the variational “savings” in the base term  $\mathcal{B}$  are strictly dominated by the misalignment penalty  $\mathcal{R}$ , effectively confining the optimization trajectory to the collinear manifold.

**A Differentiable Proxy for Group Isotopy.** This net positive coefficient ( $c_H > 0$ ) confirms that the global minima of  $\mathcal{H}$  are strictly confined to the set of group isotopes ( $\tilde{n}_v = 0$ ). This establishes  $\mathcal{H}_{\min}$  as a **differentiable proxy for group structure**.

Crucially,  $\mathcal{H}_{\min}$  is an **isotopy invariant** quantity. Detecting such intrinsic algebraic properties usually requires solving combinatorial graph isomorphism problems; remarkably, HyperCube achieves this via continuous optimization, successfully abstracting away arbitrary relabeling to detect the underlying **latent group structure** encoded in the data.

**Remark: Breaking Isotopy Symmetry.** While  $\mathcal{H}$  is invariant under the full isotopy group ( $S_n \times S_n \times S_n$ ), practical applications often require recovering the canonical group operation (e.g., to derive equivariant layers). As shown in Huh (2025), this ambiguity can be resolved by enforcing the parameter tying constraint  $A_g = B_g = C_g^\dagger, \forall g \in Q$ . This constraint breaks the isotopy symmetry down to isomorphism symmetry, forcing the model to align the identity element and recover the specific group table structure.

## Appendix C. Formal Definitions: Support Hypergraphs and Connectivity

To facilitate the understanding of the topological structure of algebraic operations within the HyperCube framework, we provide the following formal definitions.

### C.1. Support of a 3rd-Order Tensor

Given a 3rd-order tensor  $\delta \in \mathbb{R}^{n \times n \times n}$  representing a binary operation  $a \circ b = c$ , the **support** of  $\delta$  is defined as the set of indices corresponding to non-zero entries:

$$\text{supp}(\delta) = \{(a, b, c) \in [n]^3 \mid \delta_{abc} \neq 0\}$$

In the context of the HyperCube framework, the entries  $\delta_{abc}$  approach a binary state  $\{0, 1\}$ , where 1 indicates the presence of a valid operation triplet in the discovered algebra.

### C.2. Support Hypergraph

The **support hypergraph**  $H_\delta = (V, E)$  is a directed 3-uniform hypergraph constructed from  $\text{supp}(\delta)$  such that:

- $V = \{1, 2, \dots, n\}$  is the set of vertices, representing the elements of the algebra.
- $E = \{(a, b, c) \mid (a, b, c) \in \text{supp}(\delta)\}$  is the set of directed hyperedges. Each hyperedge connects an ordered triplet of vertices  $(a, b, c)$ , representing the relationship  $a \circ b = c$ .

### C.3. Hypergraph Connectedness

Connectedness in  $H_\delta$  determines the global reachability of elements through the binary operation.

- **Adjacency:** Two hyperedges  $e_i, e_j \in E$  are adjacent if they share at least one vertex ( $e_i \cap e_j \neq \emptyset$ ).
- **Path:** A path between two vertices  $u, v \in V$  is a sequence of vertices and hyperedges  $v_0, e_1, v_1, e_2, \dots, e_k, v_k$  such that  $v_0 = u, v_k = v$ , and for each  $i$ ,  $\{v_{i-1}, v_i\} \subseteq e_i$ .
- **Connectedness:**  $H_\delta$  is connected if there exists a path between every pair of vertices in  $V$ . In the case of a quasigroup, the support hypergraph is strongly connected, ensuring that the inductive distillation process can propagate information across the entire domain.

## Appendix D. Deferred Proofs

**Proof [Lemma 5: Synchronization]** Since the factorization is unitary, the slices  $A_e, B_e$  are unitary matrices. We explicitly define the gauge as  $(U, V, W) := (A_e^\dagger, I_n, B_e)$ . Under perfect collinearity and unitarity ( $|T_{abc}| = \|A\| = \|B\| = \|C\| = 1$ ), the identity  $A_a B_b \propto C_c^\dagger$  holds with unit scalars. Applying this to triples  $(g, e, g)$  and  $(e, g, g)$  yields  $A_g B_e = C_g^\dagger$  and  $A_e B_g = C_g^\dagger$ , implying  $A_g B_e = A_e B_g$ . Applying the gauge transformation:

$$A'_g = A_e^\dagger A_g = A_e^\dagger (A_e B_g B_e^\dagger) = B_g B_e^\dagger = B'_g.$$

For the third factor:

$$C'_g = B_e C_g A_e = B_e (B_e^\dagger A_g^\dagger) A_e = A_g^\dagger A_e = (A'_g)^\dagger.$$

Thus, all three factors collapse to a single unitary map  $\rho(g)$ . ■

**Proof [Lemma 11: Normalized Rank  $\kappa$ ]** Fix a supported triple  $(a, b, c)$ . Starting from  $X = C_c^\dagger C_c / \|C_c\|^2$  and substituting the collinear relation  $C_c^\dagger \propto A_a B_b$  from (8) and the Gram identity for  $Y$  from (11):

$$X = \frac{\|C_c\|^2}{|T_{abc}|^2} (A_a B_b) (B_b^\dagger A_a^\dagger) = \frac{\|B_b\|^2 \|C_c\|^2}{|T_{abc}|^2} A_a \left( \frac{B_b B_b^\dagger}{\|B_b\|^2} \right) A_a^\dagger = \frac{\|B_b\|^2 \|C_c\|^2}{|T_{abc}|^2} \frac{A_a (A_a^\dagger A_a) A_a^\dagger}{\|A_a\|^2} = \kappa_{abc} X^2.$$

Since  $X$  is index-independent, the coefficient  $\kappa_{abc}$  must be a constant  $\kappa$ . Define  $P := \kappa X$ . Then  $P^2 = \kappa^2 X^2 = \kappa X = P$ , making  $P$  an orthogonal projection. Thus,  $\text{rank}(X) = \text{rank}(P) =$

$\text{Tr}(P) = \kappa \text{Tr}(X) = \kappa n$ . Rearranging yields  $\kappa = \text{rank}(X)/n \leq 1$ . If  $\kappa = 1$ , then  $X$  is a trace- $n$  projection, implying  $X = I_n$ .  $\blacksquare$

**Proof [Lemma 15: Feasibility]** We construct a solution using canonical basis matrices  $E_{ij}$ , where  $(E_{ij})_{uv} = 1$  if  $u = i, v = j$  and 0 otherwise. Set  $A_a = E_{a1}$ ,  $B_b = E_{1b}$ , and  $C_c = n \delta_{::c}^\top$ . Note that  $A_a B_b = E_{a1} E_{1b} = E_{ab}$ , and the trace operation extracts the  $(b, a)$ -th entry:  $\text{Tr}(E_{ab} C_c) = (C_c)_{ba}$ . Therefore, the product (3) reduces to  $T_{abc}(\Theta) = \frac{1}{n} \text{Tr}(E_{ab} C_c) = \frac{1}{n} (C_c)_{ba} = \frac{1}{n} (n \delta_{::c}^\top)_{ba} = \delta_{abc}$ .  $\blacksquare$

**Proof [Theorem 16: Existence for Regularized Objective]** By Lemma 15,  $\mathcal{F}_\delta$  is nonempty. Since  $T(\cdot)$  is polynomial (hence continuous),  $\mathcal{F}_\delta = T^{-1}(\{\delta\})$  is closed. Let  $\{\Theta_k\} \subset \mathcal{F}_\delta$  be a minimizing sequence for  $\mathcal{H}_\epsilon$ . The regularization term  $\epsilon \|\Theta\|_F^2$  renders the objective coercive. Because  $\mathcal{H}(\Theta) \geq 0$  (sum of squared norms), we have  $\epsilon \|\Theta_k\|_F^2 \leq \mathcal{H}_\epsilon(\Theta_k)$  so  $\{\Theta_k\}$  is bounded in Frobenius norm (since  $\mathcal{H}_\epsilon(\Theta_k)$  is bounded along a minimizing sequence). In finite-dimensional Euclidean space, boundedness implies the existence of a convergent subsequence  $\Theta_{k_j} \rightarrow \Theta^*$  (Bolzano–Weierstrass). Closedness gives  $\Theta^* \in \mathcal{F}_\delta$ , and continuity of  $\mathcal{H}_\epsilon$  yields  $\mathcal{H}_\epsilon(\Theta^*) = \inf_{\Theta \in \mathcal{F}_\delta} \mathcal{H}_\epsilon(\Theta)$ .  $\blacksquare$

**Proof [Corollary 17: Consistency in the vanishing-regularization limit]** Let  $\Theta^*$  be an accumulation point, and pass to a convergent subsequence (still denoted)  $\Theta_{\epsilon_k}^* \rightarrow \Theta^*$ . Closedness of  $\mathcal{F}_\delta$  implies  $\Theta^* \in \mathcal{F}_\delta$ . Fix any  $\Theta' \in \mathcal{F}_\delta$ . By optimality of  $\Theta_{\epsilon_k}^*$ ,

$$\mathcal{H}(\Theta_{\epsilon_k}^*) + \epsilon_k \|\Theta_{\epsilon_k}^*\|_F^2 \leq \mathcal{H}(\Theta') + \epsilon_k \|\Theta'\|_F^2 \Rightarrow \mathcal{H}(\Theta_{\epsilon_k}^*) \leq \mathcal{H}(\Theta') + \epsilon_k \|\Theta'\|_F^2.$$

Taking  $k \rightarrow \infty$  and using continuity of  $\mathcal{H}$  gives  $\mathcal{H}(\Theta^*) \leq \mathcal{H}(\Theta')$ . Since  $\Theta'$  was arbitrary,  $\Theta^*$  is a global minimizer of  $\mathcal{H}$  on  $\mathcal{F}_\delta$ .  $\blacksquare$

## Appendix E. Rigidity of Associative (Group) Structure: Generalizing to Non-Unitary Collinear Factorizations

In Section 4.2, Theorem 7 established that any *unitary* collinear factorization implies the underlying operation is a group isotope, and Lemma 8 established the converse that every group isotope admits a unitary collinear factorization. Theorem 12 generalizes this result by relaxing the unitarity assumption. We prove that strict unitarity is not required to enforce associativity; rather, the geometric condition of perfect collinearity ( $\mathcal{R} = 0$ ) combined with feasibility is sufficient. Here is the restatement of Theorem 12.

**Theorem 22 (Collinearity-Associativity Equivalence)** *Let  $(Q, \circ)$  be a finite quasigroup. The feasible collinear manifold is non-empty if and only if  $(Q, \circ)$  is isotopic to a group.*

**Proof** Without loss of generality, assume  $(Q, \circ)$  is a loop with identity  $e$ . The proof is established in two directions: Necessity ( $\implies$ ) and Sufficiency ( $\impliedby$ ).

**Necessity ( $\implies$ ):** Assume the feasible collinear manifold is non-empty. Then there exists a factorization  $\Theta$  such that  $T(\Theta) = \delta$  and  $\mathcal{R}(\Theta) = 0$ .

**Step 1: Subspace Restriction.** By Lemma 10, the **normalized** Gram matrices

$$X = \frac{A_a A_a^\dagger}{\|A_a\|^2}, \quad Y = \frac{B_b B_b^\dagger}{\|B_b\|^2}, \quad \text{and} \quad Z = \frac{C_c C_c^\dagger}{\|C_c\|^2}$$

are independent of indices. Define the canonical active subspaces  $U = \text{Range}(X)$ ,  $V = \text{Range}(Y)$ , and  $W = \text{Range}(Z)$ . As shown in the unitary case, perfect collinearity implies these spaces share a common dimension  $k$ .

**Step 2: Induced Unitary Structure.** Critically, we cannot apply an arbitrary General Linear (GL) gauge transformation to normalize these operators, as non-unitary gauges destroy the collinearity condition  $\hat{A}_a \hat{B}_b \propto \hat{C}_c^\dagger$  (since the conjugate transpose  $\dagger$  is metric-dependent).

Instead, we work with the intrinsic geometry induced by collinearity. First, consider the raw restrictions of the factor slices to the active subspaces:

$$\check{A}_a : V \rightarrow U, \quad \check{B}_b : W \rightarrow V, \quad \check{C}_c : U \rightarrow W.$$

These maps are linear isomorphisms. We define the **normalized operators**  $\hat{A}_a, \hat{B}_b, \hat{C}_c$  by rescaling these restrictions by their slice norms:

$$\hat{A}_a := \frac{1}{\|A_a\|} \check{A}_a, \quad \hat{B}_b := \frac{1}{\|B_b\|} \check{B}_b, \quad \hat{C}_c := \frac{1}{\|C_c\|} \check{C}_c.$$

We invoke Lemma 11, which establishes that under perfect collinearity, the Gram matrices satisfy  $X = \kappa X^2$  (and similarly for  $Y, Z$ ). Restricted to the active subspace  $U$ , this implies  $X|_U = \frac{1}{\kappa} I_U$ . Substituting the definition of  $\hat{A}_a$  into this identity yields:

$$\hat{A}_a \hat{A}_a^\dagger = X|_U = \frac{1}{\kappa} I_U.$$

Since  $Y$  (which equates to  $A^\dagger A / \|A\|^2$  restricted to  $V$ ) also satisfies this property, we have:

$$\hat{A}_a^\dagger \hat{A}_a = Y|_V = \frac{1}{\kappa} I_V.$$

This rigorously proves that every normalized slice  $\hat{A}_a$  (and similarly  $\hat{B}_b, \hat{C}_c$ ) is a scaled unitary map (a scaled isometry between finite dimensional spaces).

**Step 3: Unitary Synchronization.** Since the normalized operators are scaled unitaries, we can normalize the identity elements using a *unitary* gauge transformation, which preserves the metric and the  $\dagger$ -collinearity condition. There exist unitary maps  $P : U \rightarrow \mathbb{C}^k, Q : V \rightarrow \mathbb{C}^k, R : W \rightarrow \mathbb{C}^k$  such that we can define the transformed parameters:

$$\tilde{A}_a = P \hat{A}_a Q^\dagger, \quad \tilde{B}_b = Q \hat{B}_b R^\dagger, \quad \tilde{C}_c = R \hat{C}_c P^\dagger$$

We fix the unitary gauges such that the identity elements are aligned to the identity matrix (up to scalar):

$$\tilde{A}_e \propto I_k, \quad \tilde{B}_e \propto I_k$$

Because  $P, Q, R$  are unitary, the collinearity condition transforms equivariantly. The condition  $\hat{A} \hat{B} \propto \hat{C}^\dagger$  becomes:

$$(P \hat{A} Q^\dagger)(Q \hat{B} R^\dagger) = P \hat{A} \hat{B} R^\dagger \propto P \hat{C}^\dagger R^\dagger = (R \hat{C} P^\dagger)^\dagger = \hat{C}^\dagger$$

Thus,  $\tilde{A}_a \tilde{B}_b \propto \tilde{C}_c^\dagger$  holds for the transformed matrices.

**Step 4: Associativity and Injectivity.** From Step 3, we have  $\tilde{A}_a \tilde{B}_b = \lambda_{abc} \tilde{C}_c^\dagger$ . Using the identity elements (where  $\tilde{A}_e = \tilde{B}_e = I$ ), we deduce  $\tilde{B}_g \propto \tilde{A}_g$ . Substituting this into the general relation yields the projective homomorphism property:

$$\tilde{A}_a \tilde{A}_b = \gamma_{a,b} \tilde{A}_{a \circ b}, \quad \text{for some } \gamma_{a,b} \in \mathbb{C}^\times.$$

This defines a homomorphism  $\phi : Q \rightarrow PGL(k, \mathbb{C})$  via  $g \mapsto [\tilde{A}_g]$ . Since  $PGL(k, \mathbb{C})$  is a group, the image  $\text{Im}(\phi)$  is associative. To prove  $Q$  is a group, we must show  $\phi$  is injective (trivial kernel).

Suppose for contradiction that  $\phi(x) = \phi(y)$  for  $x \neq y$ . Then  $\tilde{A}_x = s \tilde{A}_y$  for some scalar  $s \neq 0$ . By the feasibility constraint  $T(\Theta) = \delta$ , the model must reproduce the quasigroup table. Since  $Q$  is a quasigroup, the rows  $x$  and  $y$  are distinct permutations. There exists a column  $b$  such that  $y \circ b = c$  (implying  $\delta_{ybc} = 1$ ) but  $x \circ b \neq c$  (implying  $\delta_{xbc} = 0$ ). However, the linearity of the factorization implies:

$$T_{xbc} = \langle \tilde{A}_x^\dagger, \tilde{B}_b \tilde{C}_c \rangle = s \cdot \langle \tilde{A}_y^\dagger, \tilde{B}_b \tilde{C}_c \rangle = s \cdot T_{ybc}.$$

Substituting the target values yields  $0 = s \cdot 1$ , which implies  $s = 0$ . This contradicts the non-degeneracy of the factors ( $s \neq 0$ ). Thus,  $\phi$  must be injective. Since  $Q$  is isomorphic to a subgroup of  $PGL(k, \mathbb{C})$ ,  $(Q, \circ)$  is associative and therefore a group.

**Sufficiency ( $\Leftarrow$ ):** The converse holds by construction. Lemma 8 establishes that every group isotope admits a unitary collinear factorization, thereby ensuring the feasible collinear manifold is non-empty.  $\blacksquare$

## Appendix F. Balanced Representation and Gauge Fixing

The HyperCube architecture admits continuous groups of symmetry transformations—gauge freedoms—that leave the model output  $T(\Theta)$  invariant but complicate the analysis of the optimization landscape. This appendix develops two complementary gauge-fixing principles to resolve these symmetries, each serving a distinct theoretical purpose.

Throughout, we use the normalized Frobenius norm  $\|X\|^2 := \frac{1}{n} \text{Tr}(X^\dagger X)$ .

- **External Scalar Balancing (Global Boundedness):** A slice-wise rescaling gauge that relies solely on the fixed combinatorial support of the data tensor  $\text{supp}(\delta)$ . Because it depends only on the static data, this gauge provides a robust global mechanism to rule out scale divergence along the external slice-rescaling orbit and supports the existence argument by allowing reduction to balanced minimizing sequences (Section F.1).
- **Internal Diagonal Balancing (Local Rigidity):** A coordinate-wise rescaling gauge that preserves feasibility exactly but depends on the connectivity of the model’s internal coefficient graph  $G_\Theta$ . Because the topology of  $G_\Theta$  varies during training, this gauge serves as a local analysis tool, characterizing the spectral rigidity and stiffness of the representation in regimes where the graph is strongly connected—such as near group solutions (Section F.2).

### F.1. Scalar (external) balanced representation

For any feasible  $\Theta = (A, B, C)$  (i.e.  $T(\Theta) = \delta$ ), define the subspace of feasible log-scales

$$\mathcal{S}_\Theta = \{(x, y, z) \in \mathbb{R}^{3n} : x_a + y_b + z_c = 0, \forall (a, b, c) \in \text{supp}(\delta)\}.$$

For any  $(x, y, z) \in \mathcal{S}_\Theta$ , the scaled parameter

$$\Theta[x, y, z] := ((e^{x_a} A_a)_a, (e^{y_b} B_b)_b, (e^{z_c} C_c)_c)$$

preserves feasibility (since  $x_a + y_b + z_c = 0$  on  $\text{supp}(\delta)$  implies  $T(\Theta[x, y, z]) = T(\Theta) = \delta$ ).

**Scaling potential as  $\mathcal{H}$  along the feasible external orbit.** Define the scaling potential as the HyperCube objective evaluated along this feasibility-preserving slice-rescaling orbit:

$$\Phi_\Theta(x, y, z) := \mathcal{H}(\Theta[x, y, z]).$$

Writing  $\mathcal{H}$  in the supported-triple form and using homogeneity of the Frobenius norm,

$$\|e^{y_b} B_b e^{z_c} C_c\|^2 = e^{2(y_b+z_c)} \|B_b C_c\|^2,$$

we obtain the explicit “sum of exponentials” expression

$$\Phi_\Theta(x, y, z) = \sum_{(a,b,c) \in \text{supp}(\delta)} \left( e^{2(y_b+z_c)} \|B_b C_c\|^2 + e^{2(z_c+x_a)} \|C_c A_a\|^2 + e^{2(x_a+y_b)} \|A_a B_b\|^2 \right).$$

On  $\mathcal{S}_\Theta$  we may use  $y_b + z_c = -x_a$  etc. to rewrite

$$\Phi_\Theta(x, y, z) = \sum_{(a,b,c) \in \text{supp}(\delta)} \left( e^{-2x_a} \|B_b C_c\|^2 + e^{-2y_b} \|C_c A_a\|^2 + e^{-2z_c} \|A_a B_b\|^2 \right). \quad (19)$$

**Lemma 23 (Coercivity of the scaling potential)** *Assume  $\Theta$  is feasible:  $T(\Theta) = \delta$ , and assume the support hypergraph of  $\delta$  is connected (in particular, every index appears in at least one supported triple). Then for any nonzero  $u = (x, y, z) \in \mathcal{S}_\Theta$ ,*

$$\Phi_\Theta(tu) \rightarrow \infty \quad \text{as } |t| \rightarrow \infty.$$

**Proof (1) Positivity of coefficients from feasibility.** Fix  $(a, b, c) \in \text{supp}(\delta)$ , so  $\delta_{abc} = 1$  and hence

$$1 = T_{abc}(\Theta) = \frac{1}{n} \text{Tr}(A_a B_b C_c).$$

If (say)  $B_b C_c = 0$ , then  $\text{Tr}(A_a B_b C_c) = 0$ , contradicting  $T_{abc} = 1$ . Thus  $\|B_b C_c\|^2 > 0$  for every supported triple, and similarly  $\|C_c A_a\|^2 > 0$  and  $\|A_a B_b\|^2 > 0$ .

**(2) Coercivity on  $\mathcal{S}_\Theta$ .** Let  $u = (x, y, z) \in \mathcal{S}_\Theta$  be nonzero. If all components of  $u$  were  $\geq 0$ , then for every supported triple  $x_a + y_b + z_c = 0$  would force  $x_a = y_b = z_c = 0$  on that triple. By connectedness of the support, this propagates to all indices and implies  $u = 0$ , contradiction. Hence  $u$  has at least one negative component, say  $u_i < 0$ . The corresponding term in (19) contains a factor  $e^{-2tu_i} \rightarrow \infty$  as  $t \rightarrow +\infty$ , multiplied by a strictly positive coefficient, so  $\Phi_\Theta(tu) \rightarrow \infty$ . Applying the same argument to  $-u$  gives divergence as  $t \rightarrow -\infty$ .  $\blacksquare$

**Clarification (log-gauge rays, not linear parameter scaling).** In Lemma 23 (and throughout Appendix C.1), the notation  $\Phi_\Theta(tu)$  means evaluating the objective  $H$  along a *feasible slice-wise multiplicative rescaling orbit* through  $\Theta$ , parameterized in *log-scales*. Writing  $u = (x, y, z)$  with  $x, y, z \in \mathbb{R}^n$ , we set

$$tu := (tx, ty, tz), \quad \Theta[tu] := \Theta[tx, ty, tz] = ((e^{tx_a} A_a)_a, (e^{ty_b} B_b)_b, (e^{tz_c} C_c)_c).$$

Feasibility is preserved because  $u \in \mathcal{S}_\Theta$  implies  $x_a + y_b + z_c = 0$  on  $\text{supp}(\delta)$ , hence  $T(\Theta[tu]) = T(\Theta) = \delta$  for all  $t$ . This should not be confused with the *linear scaling*  $\Theta \mapsto t\Theta$  (i.e. scaling all factors by  $t$ ), which generally breaks feasibility (indeed  $T(t\Theta) = t^3 T(\Theta)$ ).

**Lemma 24 (Existence, uniqueness, and continuity of the balanced representative)** *Assume the support hypergraph of  $\delta$  is connected and  $\Theta$  is feasible. Then  $\Phi_\Theta$  is strictly convex and coercive on  $\mathcal{S}_\Theta$ . Hence  $\Phi_\Theta$  has a unique minimizer  $u^*(\Theta)$  on  $\mathcal{S}_\Theta$ . Moreover, the map  $\Theta \mapsto \tilde{\Theta} := \Theta[u^*(\Theta)]$  is continuous on the feasible set.*

**Proof Strict convexity.** On  $\mathcal{S}_\Theta$ , (19) can be regrouped as

$$\Phi_\Theta(x, y, z) = \sum_a \alpha_a e^{-2x_a} + \sum_b \beta_b e^{-2y_b} + \sum_c \gamma_c e^{-2z_c},$$

where

$$\alpha_a := \sum_{(b,c): \delta_{abc}=1} \|B_b C_c\|^2, \quad \beta_b := \sum_{(c,a): \delta_{abc}=1} \|C_c A_a\|^2, \quad \gamma_c := \sum_{(a,b): \delta_{abc}=1} \|A_a B_b\|^2.$$

By Lemma 23(1), every summand in these definitions is strictly positive, hence  $\alpha_a, \beta_b, \gamma_c > 0$ . Therefore, the Hessian of the (separable) extension of  $\Phi_\Theta$  to  $\mathbb{R}^{3n}$  is diagonal with strictly positive entries, and its restriction to the subspace  $\mathcal{S}_\Theta$  is positive definite. Thus  $\Phi_\Theta$  is strictly convex on  $\mathcal{S}_\Theta$ .

**Existence and uniqueness.** Coercivity on  $\mathcal{S}_\Theta$  is Lemma 23. Since  $\Phi_\Theta$  is continuous and coercive on the closed set  $\mathcal{S}_\Theta$ , it attains a minimizer; strict convexity implies the minimizer is unique.

**Continuity.**  $\Phi_\Theta$  depends continuously on  $\Theta$  through the coefficients  $\|B_b C_c\|^2, \|C_c A_a\|^2, \|A_a B_b\|^2$ . Since  $\Phi_\Theta$  is strictly convex and coercive on  $\mathcal{S}_\Theta$ , the argmin is single-valued; continuity of the argmin map follows from standard results (e.g. Rockafellar–Wets, *Variational Analysis*, §7.17).  $\blacksquare$

**Remark 25 (How Appendix F.1 interfaces with the existence argument in the main paper)**

Scalar balancing fixes the non-compact external slice-rescaling directions in a way that is robust because the constraint subspace  $\mathcal{S}_\Theta$  depends only on the fixed support  $\text{supp}(\delta)$ . In the main body, this permits reduction to balanced minimizing sequences. While this effectively bounds the representation scales along external orbits, we rely on the regularization argument in the main body to formally control remaining internal parameter trade-offs (whose local geometry is further detailed in Appendix F.2) and guarantee the existence of minimizers.

## F.2. Diagonal internal-gauge balanced representation

While external balancing handles global scale divergence, it does not control the internal basis alignment. Here, we introduce a complementary mechanism acting on the *internal* coordinates  $(I, J, K)$  of the HyperCube trace contraction. We restrict attention to *diagonal* (coordinate-wise) changes of the internal basis.

This diagonal internal gauge is a different (internal) feasibility-preserving symmetry than external slice-wise rescaling. Unlike external rescaling, it preserves each triple trace  $\text{Tr}(A_a B_b C_c)$  *without imposing any constraint subspace*. Consequently, feasibility  $T(\Theta) = \delta$  is preserved automatically along this gauge orbit.

**Scope and caveat (Local Rigidity vs. Global Existence).** Unlike external balancing, the key coefficients in the diagonal-gauge potential are *parameter dependent*: the weights  $W^{AB}(\Theta), W^{BC}(\Theta), W^{CA}(\Theta)$  (and thus the induced coefficient graph  $G_\Theta$ ) are functions of  $\Theta$ . Consequently, graph connectivity is a *regime condition*: it can fail if the representation becomes reducible (e.g., develops a block structure) or if certain product entries vanish.

For this reason, we view diagonal internal balancing primarily as a *local rigidity* tool. It explains why group solutions exhibit stiff internal geometry—characterized by the spectral gap of the Laplacian Hessian derived below—in regimes near the regular representation, rather than serving as a standalone global compactness mechanism.

### F.2.1. DIAGONAL INTERNAL GAUGE PRESERVES THE PRODUCT TENSOR

Let  $p, q, r \in \mathbb{R}^n$ , and define diagonal matrices

$$D_I(p) := \text{diag}(e^{p_1}, \dots, e^{p_n}), \quad D_J(q) := \text{diag}(e^{q_1}, \dots, e^{q_n}), \quad D_K(r) := \text{diag}(e^{r_1}, \dots, e^{r_n}).$$

Given  $\Theta = (A, B, C)$ , define the diagonal-gauge transform

$$A_a^{(p,q,r)} := D_K(r)^{-1} A_a D_I(p), \quad B_b^{(p,q,r)} := D_I(p)^{-1} B_b D_J(q), \quad C_c^{(p,q,r)} := D_J(q)^{-1} C_c D_K(r). \quad (20)$$

Let  $\Theta^{(p,q,r)} := (A^{(p,q,r)}, B^{(p,q,r)}, C^{(p,q,r)})$  denote the transformed parameters.

**Lemma 26 (Feasibility invariance under diagonal internal gauge)** *For every  $a, b, c$ , one has*

$$\text{Tr}(A_a^{(p,q,r)} B_b^{(p,q,r)} C_c^{(p,q,r)}) = \text{Tr}(A_a B_b C_c).$$

Consequently,  $T(\Theta^{(p,q,r)}) = T(\Theta)$ , and hence if  $\Theta \in \mathcal{F}_\delta$  then  $\Theta^{(p,q,r)} \in \mathcal{F}_\delta$  for all  $(p, q, r) \in \mathbb{R}^{3n}$ .

**Proof** Multiply the gauged slices:

$$\begin{aligned} A_a^{(p,q,r)} B_b^{(p,q,r)} C_c^{(p,q,r)} &= D_K(r)^{-1} A_a D_I(p) \cdot D_I(p)^{-1} B_b D_J(q) \cdot D_J(q)^{-1} C_c D_K(r) \\ &= D_K(r)^{-1} (A_a B_b C_c) D_K(r). \end{aligned}$$

By cyclicity of trace,  $\text{Tr}(D_K^{-1} X D_K) = \text{Tr}(X)$ , giving the claim. ■

**Remark 27 (Residual gauge direction)** *The transformation (20) is invariant under the common shift  $(p, q, r) \mapsto (p + t\mathbf{1}, q + t\mathbf{1}, r + t\mathbf{1})$  since  $D_I(p + t\mathbf{1}) = e^t D_I(p)$  etc., and the scalar  $e^t$  cancels in (20). Thus the diagonal gauge orbit is parameterized by  $(p, q, r)$  modulo the one-dimensional subspace  $\text{span}\{(\mathbf{1}, \mathbf{1}, \mathbf{1})\}$ .*

### F.2.2. DIAGONAL-GAUGE SCALING POTENTIAL

Define the diagonal-gauge scaling potential as the HyperCube objective along the diagonal orbit:

$$\Psi_{\Theta}(p, q, r) := H\left(\Theta^{(p,q,r)}\right). \quad (21)$$

We first record an entrywise identity for diagonal scalings. For diagonal  $D_1 = \text{Diag}(e^{u_1}, \dots, e^{u_n})$ ,  $D_2 = \text{Diag}(e^{v_1}, \dots, e^{v_n})$  and any  $X \in \mathbb{C}^{n \times n}$ ,

$$\|D_1^{-1}XD_2\|^2 = \frac{1}{n} \sum_{\alpha, \beta=1}^n e^{-2u_\alpha} e^{2v_\beta} |X_{\alpha\beta}|^2. \quad (22)$$

Using the gauge identities

$$\begin{aligned} A_a^{(p,q,r)} B_b^{(p,q,r)} &= D_K(r)^{-1} (A_a B_b) D_J(q), \\ B_b^{(p,q,r)} C_c^{(p,q,r)} &= D_I(p)^{-1} (B_b C_c) D_K(r), \\ C_c^{(p,q,r)} A_a^{(p,q,r)} &= D_J(q)^{-1} (C_c A_a) D_I(p), \end{aligned}$$

and expanding by (22), we obtain a compact “sum of exponentials” form.

**Definition 28 (Diagonal coefficient weights)** *For  $\Theta = (A, B, C)$  define nonnegative coefficient matrices*

$$W_{uv}^{AB}(\Theta) := \frac{1}{n} \sum_{a,b} |(A_a B_b)_{uv}|^2, \quad (u \in K, v \in J), \quad (23)$$

$$W_{uv}^{BC}(\Theta) := \frac{1}{n} \sum_{b,c} |(B_b C_c)_{uv}|^2, \quad (u \in I, v \in K), \quad (24)$$

$$W_{uv}^{CA}(\Theta) := \frac{1}{n} \sum_{c,a} |(C_c A_a)_{uv}|^2, \quad (u \in J, v \in I). \quad (25)$$

**Lemma 29 (Explicit diagonal-gauge potential)** *With weights (23)–(25), the diagonal-gauge potential is*

$$\Psi_{\Theta}(p, q, r) = \sum_{u,v} W_{uv}^{AB}(\Theta) e^{2(q_v - r_u)} + \sum_{u,v} W_{uv}^{BC}(\Theta) e^{2(r_v - p_u)} + \sum_{u,v} W_{uv}^{CA}(\Theta) e^{2(p_v - q_u)}. \quad (26)$$

**Proof** Apply (22) to each pairwise product term in  $H(\Theta^{(p,q,r)})$ , then sum over external indices. The coefficients aggregate exactly into  $W^{AB}, W^{BC}, W^{CA}$  as defined.  $\blacksquare$

### F.2.3. COEFFICIENT GRAPH AND LAPLACIAN HESSIAN

Equation (26) is naturally an “exponential edge energy” on a directed tripartite graph.

**Definition 30 (Directed coefficient graph)** Let  $V := I \sqcup J \sqcup K$  with  $|I| = |J| = |K| = n$ . Define a directed weighted graph  $G_\Theta = (V, E, w)$  by including edges

$$\begin{aligned} K_u \rightarrow J_v \text{ with weight } w_{K_u \rightarrow J_v} := W_{uv}^{AB}(\Theta), \\ I_u \rightarrow K_v \text{ with weight } w_{I_u \rightarrow K_v} := W_{uv}^{BC}(\Theta), \\ J_u \rightarrow I_v \text{ with weight } w_{J_u \rightarrow I_v} := W_{uv}^{CA}(\Theta), \end{aligned}$$

whenever the corresponding weight is positive. Identify  $(p, q, r) \in \mathbb{R}^{3n}$  with a node-potential  $x \in \mathbb{R}^V$  via  $x_{I_u} = p_u$ ,  $x_{J_u} = q_u$ ,  $x_{K_u} = r_u$ . For an edge  $e = (u \rightarrow v)$  define

$$\phi_e(x) := w_e e^{2(x_v - x_u)}. \quad (27)$$

Then  $\Psi_\Theta(x) = \sum_{e \in E} \phi_e(x)$ .

**Remark 31 (Regime dependence of  $G_\Theta$ )** The edge set  $E = \{w_e > 0\}$  is determined by the vanishing/nonvanishing pattern of the weights  $W^{AB}(\Theta)$ ,  $W^{BC}(\Theta)$ ,  $W^{CA}(\Theta)$  and can change with  $\Theta$ . As a result, graph connectivity properties (and the nullspace of the Laplacian Hessian below) are best interpreted locally on regions of parameter space where the positivity pattern is stable.

**Lemma 32 (Laplacian Hessian)** Let  $B \in \mathbb{R}^{E \times V}$  be the oriented incidence matrix whose row for  $e = (u \rightarrow v)$  is  $b_e := \mathbf{e}_v - \mathbf{e}_u$ . Then for all  $x \in \mathbb{R}^V$ ,

$$\nabla^2 \Psi_\Theta(x) = 4 B^\top \text{Diag}(\phi_e(x)) B. \quad (28)$$

Equivalently, defining the (undirected) weighted Laplacian  $L_\phi(x) := B^\top \text{Diag}(\phi_e(x)) B$ , we have

$$z^\top L_\phi(x) z = \sum_{e=(u \rightarrow v) \in E} \phi_e(x) (z_v - z_u)^2 \quad \forall z \in \mathbb{R}^V.$$

**Proof** For a single edge term  $\phi_e(x) = w_e e^{2(x_v - x_u)}$ ,

$$\partial_{x_u} \phi_e = -2\phi_e, \quad \partial_{x_v} \phi_e = +2\phi_e,$$

and the only nonzero second derivatives are

$$\partial_{x_u x_u} \phi_e = 4\phi_e, \quad \partial_{x_v x_v} \phi_e = 4\phi_e, \quad \partial_{x_u x_v} \phi_e = \partial_{x_v x_u} \phi_e = -4\phi_e.$$

This equals  $4\phi_e b_e b_e^\top$ . Summing over edges yields  $\nabla^2 \Psi_\Theta(x) = 4 \sum_e \phi_e b_e b_e^\top = 4B^\top \text{Diag}(\phi_e) B$ . The quadratic form identity follows immediately.  $\blacksquare$

**Corollary 33 (Convexity and the constant null direction)** For every  $x$ ,  $\nabla^2 \Psi_\Theta(x) \succeq 0$ . Moreover,  $\Psi_\Theta$  is invariant under  $x \mapsto x + t\mathbf{1}_V$ , hence  $L_\phi(x)\mathbf{1}_V = 0$  and  $\mathbf{1}_V \in \ker(\nabla^2 \Psi_\Theta(x))$ . If the underlying undirected graph of  $G_\Theta$  is connected, then  $\ker(L_\phi(x)) = \text{span}\{\mathbf{1}_V\}$  and  $\Psi_\Theta$  is strictly convex on any affine gauge slice transverse to  $\mathbf{1}_V$ , e.g.

$$\mathcal{S}_{\text{diag}} := \left\{ x \in \mathbb{R}^V : \sum_{v \in V} x_v = 0 \right\}.$$

## F.2.4. COERCIVITY IN A STRONGLY CONNECTED SPECIAL CASE

Strict convexity modulo constants does *not* by itself imply coercivity for sums of directed exponentials. A clean obstruction is the existence of a nonconstant potential which is nonincreasing along all directed edges. This obstruction is ruled out if the directed coefficient graph is strongly connected.

**Assumption 34 (Strong connectivity of the diagonal coefficient graph)** *The directed graph  $G_\Theta$  induced by the positive-weight edges in Definition 30 is strongly connected. A sufficient (very special) condition is full support:  $W_{uv}^{AB}(\Theta) > 0$ ,  $W_{uv}^{BC}(\Theta) > 0$ , and  $W_{uv}^{CA}(\Theta) > 0$  for all  $u, v$ .*

**Remark 35 (Why Assumption 34 is a special-case hypothesis)** *Assumption 34 is a regime condition rather than a structural property of the constraint  $\delta$ : the weights are functions of  $\Theta$  and may lose support (e.g. under reducible or structurally sparse product patterns). When strong connectivity fails, the Laplacian kernel can grow beyond  $\text{span}\{\mathbf{1}_V\}$ , and coercivity/uniqueness on  $\mathcal{S}_{\text{diag}}$  can fail.*

**Lemma 36 (Coercivity on the gauge slice for strongly connected diagonal coefficient graph)**

*Under Assumption 34,  $\Psi_\Theta$  is coercive on  $\mathcal{S}_{\text{diag}}$ . Equivalently, for every nonzero  $u \in \mathcal{S}_{\text{diag}}$ ,*

$$\Psi_\Theta(tu) \rightarrow \infty \quad \text{as } |t| \rightarrow \infty.$$

**Proof** Fix nonzero  $x \in \mathcal{S}_{\text{diag}}$  and write  $d_e := x_v - x_u$  for each directed edge  $e = (u \rightarrow v)$ . If  $d_e \leq 0$  for every edge  $e$  with  $w_e > 0$ , then along every directed path  $v_0 \rightarrow v_1 \rightarrow \dots \rightarrow v_m$  we have  $x_{v_m} - x_{v_0} = \sum_{\ell=0}^{m-1} d_{(v_\ell \rightarrow v_{\ell+1})} \leq 0$ . By strong connectivity, for any two nodes  $s, t$  there exist directed paths  $s \rightarrow t$  and  $t \rightarrow s$ , so  $x_t - x_s \leq 0$  and  $x_s - x_t \leq 0$ , implying  $x_s = x_t$ . Thus  $x$  must be constant on  $V$ , hence  $x = 0$  on  $\mathcal{S}_{\text{diag}}$ , contradiction. Therefore, there exists at least one directed edge  $e$  with  $w_e > 0$  and  $d_e > 0$ . For that edge,

$$\Psi_\Theta(tx) \geq \phi_e(tx) = w_e e^{2td_e} \xrightarrow[t \rightarrow \infty]{} \infty.$$

Finally, applying the same argument to  $-x \in \mathcal{S}_{\text{diag}}$  yields divergence as  $t \rightarrow -\infty$ . ■

**Clarification (diagonal internal gauge rays).** Likewise, in Lemma 36 the expression  $\Psi_\Theta(tu)$  denotes  $H$  evaluated along the *diagonal internal-gauge orbit*. Writing  $u = (p, q, r) \in \mathcal{S}_{\text{diag}}$  and  $tu = (tp, tq, tr)$ , we evaluate

$$\Psi_\Theta(tu) = H\left(\Theta^{(tp, tq, tr)}\right),$$

where  $\Theta^{(p, q, r)}$  is the diagonal-gauge transform from (20). By Lemma 26, this gauge transform preserves feasibility via cyclicity of trace, i.e.  $T(\Theta^{(p, q, r)}) = T(\Theta)$  for all  $(p, q, r)$ , but it typically changes the objective  $H$ . Moreover,  $\Psi_\Theta(tu)$  has the explicit “sum of exponentials” form in (26) (an exponential edge-energy on the coefficient graph), and therefore should not be interpreted as a quadratic function of  $t$  (in particular,  $\Psi_\Theta(tu) \neq t^2 \Psi_\Theta(u)$  in general). The divergence  $\Psi_\Theta(tu) \rightarrow \infty$  as  $|t| \rightarrow \infty$  is a nontrivial statement that uses graph connectivity properties.

## F.2.5. EXISTENCE AND UNIQUENESS OF A DIAGONAL-BALANCED REPRESENTATIVE

**Lemma 37 (Existence, uniqueness, and continuity (special case))** *Assume Assumption 34 holds. Then  $\Psi_\Theta$  is strictly convex and coercive on  $\mathcal{S}_{\text{diag}}$ . Hence it admits a unique minimizer  $x^*(\Theta) \in \mathcal{S}_{\text{diag}}$ . Define the diagonal-balanced representative by*

$$\Theta^{\text{diag}} := \Theta^{(p^*, q^*, r^*)}, \quad \text{where } x^* = (p^*, q^*, r^*).$$

*Moreover, the map  $\Theta \mapsto x^*(\Theta)$  (and thus  $\Theta \mapsto \Theta^{\text{diag}}$ ) is continuous on any set where the coefficient weights in Definition 28 vary continuously and remain in the same strong-connectivity regime.*

**Proof** Strong connectivity implies the underlying undirected graph is connected, so strict convexity on  $\mathcal{S}_{\text{diag}}$  follows from Corollary 33. Coercivity on  $\mathcal{S}_{\text{diag}}$  is Lemma 36. Thus  $\Psi_\Theta$  has a unique minimizer on  $\mathcal{S}_{\text{diag}}$ . Continuity of the argmin map follows from standard stability results for strictly convex coercive objectives under continuous perturbations of the coefficients, as long as the positivity pattern (hence strong-connectivity regime) does not change. ■

**Remark 38 (Coefficient weights, coefficient graph, and strong connectivity)** *Recall the diagonal coefficient weights (Defs. (23)–(25)):*

$$W_{uv}^{AB}(\Theta) = \frac{1}{n} \sum_{a,b} |(A_a B_b)_{uv}|^2, \quad W_{uv}^{BC}(\Theta) = \frac{1}{n} \sum_{b,c} |(B_b C_c)_{uv}|^2, \quad W_{uv}^{CA}(\Theta) = \frac{1}{n} \sum_{c,a} |(C_c A_a)_{uv}|^2.$$

*Thus  $W_{uv}^{AB}(\Theta) > 0$  iff some pair  $(a, b)$  yields a nonzero entry  $(A_a B_b)_{uv}$ ; equivalently, the learned families of pairwise products ever couple internal coordinate  $u$  to  $v$ . The directed coefficient graph  $G_\Theta$  is the tripartite encoding of these nonzero couplings.*

*Assumption 34 (strong connectivity) rules out internal decompositions into noninteracting coordinate clusters: for any  $s, t \in V = I \sqcup J \sqcup K$ , there exists an alternating directed path from  $s$  to  $t$  using only positive-weight edges. When strong connectivity fails, the representation becomes reducible in the chosen internal basis, and diagonal internal balancing can lose coercivity/uniqueness (as reflected by growth of the Laplacian kernel and collapse of the spectral gap).*

**Remark 39 (Diagonal internal gauge: energy barrier and canonical representative)** *The diagonal internal gauge  $(p, q, r)$  (Eq. (20)) preserves feasibility exactly:  $T(\Theta^{(p,q,r)}) = T(\Theta)$ , so it is a genuine non-compact reparameterization direction of the constraint set  $\mathcal{F}_\delta$ . However,  $H$  is generally not invariant under these non-unitary scalings, and the diagonal-gauge potential*

$$\Psi_\Theta(p, q, r) := H(\Theta^{(p,q,r)})$$

*measures the cost of drifting along a feasible internal scaling orbit.*

*Under Assumption 34, Lemma 36 shows coercivity on the gauge slice  $\mathcal{S}_{\text{diag}}$ : for every nontrivial  $u \in \mathcal{S}_{\text{diag}}$ ,*

$$\Psi_\Theta(tu) \rightarrow \infty \quad \text{as } |t| \rightarrow \infty,$$

*so runaway coordinate-wise internal rescalings are impossible at bounded cost.*

*Combining coercivity with strict convexity modulo constants (Cor. 33) yields a unique minimizer of  $\Psi_\Theta$  on  $\mathcal{S}_{\text{diag}}$  (Lemma 37), defining a canonical diagonal-balanced representative  $\Theta^{\text{diag}}$  along the diagonal-gauge orbit.*

**Remark 40 (Regular-representation regime implies full support)** *At the regular-representation certificate for groups, each product slice  $A_a B_b$  is a permutation matrix. Consequently  $\sum_{a,b} |(A_a B_b)_{uv}|^2 = n$  for all  $u, v$ , so  $W_{uv}^{AB} = 1$  for all  $u, v$  (and similarly  $W_{uv}^{BC} = W_{uv}^{CA} = 1$ ). Hence  $G_\Theta$  is complete tripartite and strongly connected, and the diagonal-balanced representative is well-defined and unique in this regime.*

**Remark 41 (Spectral gap controls local conditioning)** *At any  $x \in \mathcal{S}_{\text{diag}}$ , the Hessian of  $\Psi_\Theta$  has Laplacian form (Lemma 32); thus the strong convexity modulus of  $\Psi_\Theta$  restricted to  $\mathcal{S}_{\text{diag}}$  is governed by the Laplacian spectral gap  $\lambda_2(L_\phi(x))$ . This yields a quantitative local “spectral rigidity” principle whenever the coefficient graph remains connected/strongly connected. If edges vanish and the graph becomes (reducibly) disconnected,  $\lambda_2$  can collapse and the rigidity/conditioning control is lost.*

**Remark 42 (How Appendix F.2 should be used in the main text)** *External (slice) balancing addresses non-compact scale trade-offs tied to the fixed support  $\text{supp}(\delta)$  and is the right tool for reducing existence/compactness questions to a bounded balanced set.*

*Diagonal internal balancing instead probes a different family of non-unitary internal directions. Near high-rank group solutions (Remark 40), it explains why the objective exhibits stiff internal geometry (Laplacian Hessian / spectral gap), and should be viewed primarily as a local stability/rigidity tool rather than a standalone global coercivity mechanism.*

## Appendix G. Discussion on Coercivity

**Geometric obstructions to a direct unregularized existence proof.** A general proof that the unregularized infimum in (15) is attained (e.g., via coercivity modulo gauge) faces several interlocking challenges:

- **Non-compact gauge orbits:** the model admits continuous multiplicative gauge transformations; proving compactness/coercivity in the quotient requires uniform control of these non-compact directions.
- **Subspace alignment and persistent cancellations:** high-norm “ghost modes” may, in principle, keep pairwise products bounded via aligned singular-vector projections. One must rule out such cancellations uniformly under the trilinear feasibility constraint.
- **Spectral rigidity vs. combinatorial support:** deriving uniform spectral bounds from only combinatorial hypotheses on  $\delta$  requires bridging expansion/connectedness properties with nonconvex variational analysis.

**Possible directions for a proof.** Natural ingredients (partially developed in Appendix F) include: (i) fix a canonical balanced gauge and prove compactness of the unit-scale balanced set under suitable nondegeneracy hypotheses; (ii) establish uniform spectral lower bounds on slice singular values on that compact set; (iii) use SVD/projection estimates to rule out persistent cancellations that would allow norms to diverge while pairwise products remain bounded.